การปรับปรุงสมรรถนะของเซลล์เชื้อเพลิงชนิดออกไซด์ของแข็ง

โดยใช้สแตกที่ต่อแบบอนุกรม

นายณัฐพล เรืองรัศมี

สถาบันวิทยบริการ
จุฬาลงกรณ์มหาวิทยาลัย

วิทยานิพนธ์นี้เป็นส่วนหนึ่งของการศึกษาตามหลักสูตรปริญญาวิศวกรรมศาสตรมหาบัณฑิต

สาขาวิชาวิศวกรรมเคมี ภาควิชาวิศวกรรมเคมี

คณะวิศวกรรมศาสตร์ จุฬาลงกรณ์มหาวิทยาลัย

ปีการศึกษา 2549

ลิขสิทธิ์ของจุฬาลงกรณ์มหาวิทยาลัย

IMPROVEMENT OF SOLID OXIDE FUEL CELL PERFORMANCE USING SERIALLY CONNECTED STACKS

Mr. Nattaphol Ruangrassamee

สถาบันวิทยบริการ
จุฬาลงกรณ์มหาวิทยาลัย

A Thesis Submitted in Partial Fulfillment of the Requirements
for the Degree of Master of Engineering Program in Chemical Engineering
Department of Chemical Engineering
Faculty of Engineering
Chulalongkorn University
Academic Year 2006

Copyright of Chulalongkorn University

Thesis Title	IMPROVEMENT OF SOLID OXIDE FUEL CELL PERFORMANCE USING SERIALLY CONNECTED STACKS
By	Mr. Nattaphol Ruangrassamee
Field of Study	Chemical Engineering
Thesis Advisor	Associate Professor Suttichai Assabumrungrat, Ph.D.
Thesis Co-advisor	Assistant Professor Navadol Laosiripojana, Ph.D.

Accepted by the Faculty of Engineering, Chulalongkorn University in Partial Fulfillment of the Requirements for the Master's Degree

..... Dean of the Faculty of Engineering
(Professor Direk Lavansiri, Ph.D.)

THESIS COMMITTEE

..... Chairman
(Associate Professor Prasert Pavasant, Ph.D.)

..... Thesis Advisor
(Associate Professor Suttichai Assabumrungrat, Ph.D.)

..... Thesis Co-advisor
(Assistant Professor Navadol Laosiripojana, Ph.D.)

..... Member
(Assistant Professor Bunjerd Jongsomjit, Ph.D.)

..... Member
(Amornchai Arpornwichanop, D.Eng.)

สถาบันวิทยบริการ
จุฬาลงกรณ์มหาวิทยาลัย

ณัฐพล เรืองรัศมี : การปรับปรุงสมรรถนะของเซลล์เชื้อเพลิงชนิดออกไซด์ของแข็ง โดยใช้สแตกที่ต่อแบบอนุกรม (IMPROVEMENT OF SOLID OXIDE FUEL CELL PERFORMANCE USING SERIALLY CONNECTED STACKS) อ. ที่ปรึกษา : รศ. ดร. สุทธิชัย อัสสะบำรุงรัตน์, อ. ที่ปรึกษาร่วม : ผศ. ดร. นวดล เหล่าศิริพจน์, 90 หน้า.

วิทยานิพนธ์นี้ศึกษาเพื่อหาการปรับปรุงประสิทธิภาพที่น่าจะเป็นไปได้ของระบบเซลล์เชื้อเพลิงชนิดออกไซด์ของแข็ง (SOFC) โดยใช้สแตกที่ต่อแบบอนุกรม ซึ่งความต่างศักย์ที่ใช้สามารถปรับเปลี่ยนไปได้ตามสแตกต่างๆ โดยงานนี้จะพิจารณาจากการศึกษาเชิงเปรียบเทียบระหว่างระบบการจัดเรียงเซลล์เชื้อเพลิงชนิดออกไซด์ของแข็งแบบทั่วไป ซึ่งมักจะใช้การต่อสแตกแบบขนาน กับระบบการจัดเรียงที่ได้เสนอในงานนี้ ซึ่งใช้การต่อสแตกแบบอนุกรม โดยจะพิจารณาเป็นสองกรณีด้วยกัน เช่น กรณีที่มีกับไม่มีการคิดผลของความดันลดร่วมด้วย และผลที่ได้พบว่า ระบบการจัดเรียงที่ใช้การต่อสแตกแบบอนุกรมนั้นสามารถปรับปรุงกำลังไฟฟ้าที่ได้และประสิทธิภาพได้สูงถึง 5% แต่การปรับปรุงดังกล่าวนั้นจะมีนัยสำคัญที่น้อยลง หากสแตกมีจำนวนมากกว่าสองสแตก นอกจากนี้ ยังพบอีกว่าการจัดเรียงระหว่างเซลล์เชื้อเพลิงที่ใช้การต่อสแตกแบบอนุกรม กับเครื่องคอมเพรสเซอร์แบบที่ติดตั้งไว้ที่ขาเข้าของสแตกแรกเพียงเครื่องเดียว จะเป็นตัวเลือกที่ดีที่สุด แต่อย่างไรก็ตาม เมื่อนำไปเปรียบเทียบกับกรณีของการจัดเรียงเซลล์เชื้อเพลิงแบบขนานแล้ว จะเห็นได้ว่าความดันลดที่เกิดขึ้นในกรณีของการจัดเรียงเซลล์เชื้อเพลิงแบบอนุกรมนั้น จะมีค่าประมาณ 4.7 เท่า ในส่วนของแอโนด และ 3.75 เท่า ในส่วนของแคโทด ด้วยเหตุผลนี้เอง การจัดเรียงเซลล์เชื้อเพลิงดังกล่าวนั้น จึงต้องการกำลังไฟฟ้าเพื่อการดำเนินงานเครื่องคอมเพรสเซอร์ที่สูง ซึ่งแนะนำว่าควรที่จะมีการติดตั้งระบบที่นำความร้อนกลับมาใช้ เพื่อสามารถนำไปใช้ในดำเนินการเชิงปฏิบัติได้จริง

สถาบันวิทยบริการ
จุฬาลงกรณ์มหาวิทยาลัย

ภาควิชา วิศวกรรมเคมี	ลายมือชื่อนิสิต ณัฐพล เรืองรัศมี
สาขาวิชา วิศวกรรมเคมี	ลายมือชื่ออาจารย์ที่ปรึกษา
ปีการศึกษา 2549	ลายมือชื่ออาจารย์ที่ปรึกษาร่วม
Academic year 2006	Co-advisor's signature

4870288821 : MAJOR CHEMICAL ENGINEERING
KEY WORD : SERIALLY CONNECTED STACKS / POWER GENERATION / SOLID OXIDE FUEL CELL / SIMULATION

NATTAPHOL RUANGRASSAMEE : IMPROVEMENT OF SOLID OXIDE FUEL CELL PERFORMANCE USING SERIALLY CONNECTED STACKS
THESIS ADVISOR: ASSOC. PROF. SUTTICHAI ASSABUMRUNGRAT, Ph.D.,
THESIS COADVISOR: ASST. PROF. NAVADOL LAOSIRIPOJANA, Ph.D., 90 pp.

This study was carried out to investigate the possible improvement of SOFC performance by using multiple stacks arranged in series in which the operating voltages were allowed to vary among the different stacks. The comparative study on the operation in conventional SOFC configuration in which multiple stacks are typically arranged in parallel and the alternative ones in which stacks are networked in series is considered in both case; i.e with and without considering the effect of pressure drop. By connected the stacks in series instead of in parallel, the power and electrical efficiency improvement as high as 5.0% can be achieved. Moreover, the improvement by the arrangement in series becomes less significant after the number of stacks more than 2. The configuration in series with one compressor installed only at the inlets of the first stack is the best option when taking into account the pressure drop. However, the pressure drops are about 4.7 and 3.75 times in the anodic and cathodic channels, respectively, compared with those from the case with stack arrangement in parallel. Therefore it requires higher consumption of compression power. It was suggested that, to compensate a part of power consumption from installed compressors, the heat recovery system should be installed to offer the practical operation.

สถาบันวิทยบริการ
จุฬาลงกรณ์มหาวิทยาลัย

Department ....Chemical Engineering..... Student's signature ..Nattaphol Ruangrassamee...
Field of Study ..Chemical Engineering.... Advisor's signature .....
Academic year .....2006..... Co-advisor's signature .....

ACKNOWLEDGEMENTS

The author would like to express his sincere gratitude and appreciation to his advisor, Associate Professor Suttichai Assabumrungrat, and co advisor, Assistant Professor Navadol Laosiripojana for their invaluable suggestions, stimulating, useful discussions throughout this research and devotion to revise this thesis otherwise it can not be completed in a short time. In addition, the author would also be grateful to Associate Professor Prasert Pavasant, as the chairman, and Assistant Professor Bunjerd Jungsomjit, and Dr. Amornchai Arpornwichanop as the members of the thesis committee. The financial supports from PTT Public Company Limited Graduate Scholarship and Graduate School of Chulalongkorn University are gratefully acknowledged.

Most of all, the author would like to express his highest gratitude to his parents who always pay attention to him all the times for suggestions and have provided his support and encouragement. The most success of graduation is devoted to my parents.

Finally, many thanks for kind suggestions and useful help to Mr. Supawat Vivanpatarakij, Mr. Wiboon Sangtongkitcharoen, Mr. Watcharapong Khaodee and the members of the Center of Excellence on Catalysis and Catalytic Reaction Engineering, Department of Chemical Engineering, Faculty of Engineering, Chulalongkorn University for their assistance.

ศูนย์วิทยทรัพยากร
จุฬาลงกรณ์มหาวิทยาลัย

CONTENTS

Page

ABSTRACT (IN THAI) …….. iv

ABSTRACT (IN ENGLISH) …….. v

ACKNOWLEDGEMENTS ……... vi

CONTENTS …… vii

LIST OF TABLES …….. x

LIST OF FIGURES ……..... xi

NOMENCLATURE ……..... xiii

CHAPTERS

I INTRODUCTION ……..……. 1

1.1 Motivation of the thesis.…….…….…..... 1

1.2 Objective of the work... …….…….…..... 4

II THEORY ……..... 5

2.1 Basic of fuel cells.....…….…….…..... 5

2.2 Fuel cell performance …….…….……. 8

2.2.1 Ideal performance ……...….....……...… 9

2.2.2 Actual performance.....……..... 10

2.3 Solid oxide fuel cells.. ……..……..…….. 13

III LITERATURE REVIEWS ……..……..... 17

3.1 A wide variety of fuels for solid oxide fuel cells …...……. 17

3.2 Several approaches for performance improvement of solid oxide fuel cells …….....……... 19

3.3 An interesting approach: The concept of multiple fuel cell stacks in series ….……..... 21

IV MODEL DEVELOPMENT ……...…… 22

4.1 Mathematical SOFC model ..……...…….. 22

4.1.1 Electrochemical model ……..……..... 25

CHAPTERS **Page**

4.1.2 Fuel utilization factor and fuel cell efficiency……. 26
4.1.2.1 Fuel utilization factor .....……..…….. 26
4.1.2.2 Fuel cell efficiency ……..…….…. 27
4.2 Model validation …..……..…… 28
4.3 System configuration ……..…….…… 29
V RESULTS AND DISCUSSION ……. 34
5.1 Model validation ……..…...……...… 34
5.2 Performance of single-stack SOFC and multiple stack SOFCs: Neglecting effect of pressure drop ……....……..... 35
5.2.1 Performance of the single stack SOFC ……..……..... 36
5.2.2 Performance of multiple stack SOFCs with different arrangement ……....……..... 41
5.2.3 Influence of number of connected stacks on power improvement by the arrangement in series ……... 47
5.3 Performance of SOFCs : taking into account the presence of pressure drop ……....……... 48
5.3.1 Effect of generated pressure drop on the single stack SOFC performance ……..... 48
5.3.2 Actual performance of different configurations of integrated stacks and compressors ……....……..... 51
VI CONCLUSIONS AND RECOMMENDATIONS ……. 60
6.1 Conclusions ……....….. 60
6.2 Recommendations ……....…… 61
REFERENCES …….…….... 62
APPENDICES
APPENDIX A. SELECTED THERMODYNAMIC AND TRANSPORT PROPERTY DATA ……..…….. 69
APPENDIX B. DETERMINING GIBBS ENERGY 72
APPENDIX C. EXPRESSIONS OF OVERPOTENTIALS ……..... 74

CHAPTERS **Page**

APPENDIX D. CALCULATION OF GAS PHASE
. **ISOTHERMAL PRESSURE DROP** 77
APPENDIX E. CALCULATION OF COMPRESSOR
POWER CONSUMPTION……..... 81
APPENDIX F. SEQUENCE OF THE CALCULATIONS ……..... 86
VITA ……..… 90

สถาบันวิทยบริการ
จุฬาลงกรณ์มหาวิทยาลัย

LIST OF TABLES

TABLE		Page
1.1	APEC sectored energy demand outlook from 2000 to 2020 ……..	1
2.1	Summary of major differences of the fuel cell types ……..	8
2.2	Evolution of cell component technology for solid oxide fuel cells .	16
A.1	Heat capacities of some gases .....……..... .....…….....	69
A.2	Standard heat of formation (H_f^o) and entropy (S_f^o) of some gases .	69
A.3	Lennard-Jones potential parameters …….....…….....	70
C.1	Material used and resistivity of cell component . .....…….....	76

สถาบันวิทยบริการ
จุฬาลงกรณ์มหาวิทยาลัย

LIST OF FIGURES

FIGURE		Page
2.1	Schematic of an Individual Fuel Cell .....…	5
2.2	Ideal and actual fuel cell voltage/current characteristic	11
2.3	Solid oxide fuel cell designs at the cathode …….....	13
2.4	Solid oxide fuel cell operating principle ……....….	14
4.1	The schematic diagram of a planar type SOFC stack with internal manifolds ……...……....…...	23
4.2	The typical SOFC dimensions in unit of millimeters ……....…..	24
4.3	Schematic representation of fuel flow configurations for two stacks in a) parallel b) series ……..……....…..	30
4.4	SOFC and compressor configurations for two stacks in a.) parallel with one compressor installed before SOFC system b.) series with one compressor installed before SOFC system c.) series with staged compressors installed with every stacks …….....	33
5.1	Characteristic curves of SOFC (pure hydrogen as fuel and air as oxidant at fuel utilization = 80% and temperature = 1173 K) ..…….	35
5.2	Effects of methane feed rate and operating voltage on generated power in single SOFC stack (assuming no generated pressure drop)	38
5.3	Effects of methane feed rate and operating voltage on electrical efficiency in single SOFC stack (assuming no generated pressure drop) ……....…..	39
5.4	Effects of methane feed rate and operating voltage on fuel utilization in single SOFC stack (assuming no generated pressure drop …….……	40
5.5	Relationship of operating voltage in each stack on generated power for arrangement in series and parallel of 2 stacks …….....	42
5.6	Relationship of operating voltage in each stack on electrical efficiency for arrangement in series and parallel of 2 stacks ……..	43

FIGURE **Page**

5.7	Relationship of operating voltage in each stack on fuel utilization arrangement in series and parallel of 2 stacks ……..…..	44
5.8	Relationship of operating voltage in each stack of arrangement in series on split fraction of fuel utilization ……..…..	46
5.9	Effect of the number of stacks on the power improvement ……..…..	47
5.10	Effect of operating voltage and methane feed rate on generated pressure drop in the anodic and cathodic channels of the single stack ...	49
5.11	Effect of operating voltage and methane feed rate on generated power from SOFC and power consumption from compressors in single stack .	50
5.12	Relationship of operating voltage in each stack on generated power for 2 stacks in different configurations …...……..…..	52
5.13	Relationship of operating voltage in each stack on electrical efficiency for 2 stacks in different configurations …….…..	53
5.14	Relationship of operating voltage in each stack on fuel utilization for 2 stacks in different configurations ...…….……..…..	54
5.15	Effect of operating voltage in each stack on generated pressure drop in anodic and cathodic channel in different configurations …..…..	56
5.16	Relationship of operating voltage in each stack on power consumption from compressors for 2 stacks in different configurations …...……..…..	57
5.17	Relationship of operating voltage in each stack on the obtained net power for 2 stacks in different configurations …….……	58
D.1	The energy balance in any cell channel ...……....….	77
E.1	Symbol used for compressors	81

NOMENCLATURE

a	First ohmic resistance constant as shown in Eq.(C.7)	[Ω m]
A	Cell Area	[m^2]
b	Second ohmic resistant constant as shown in Eq.(C.7)	[K]
E_0	Open circuit voltage	[V]
F	Faraday constant (96485.34)	[C mol^{-1}]
i	Current density	[A m^{-2}]
LHV	Lower heating value of methane feed	[W]
m	Constant polarization parameters	[-]
p	Partial pressure	[atm]
P	Power	[kW]
r	Activation polarization parameters	[A m^{-2}]
R	Universal gas constant ($8.31447x10^{-3}$)	[kJ mol^{-1} K^{-1}]
T	Absolute temperature	[K]
U_f	Fuel utilization	[%]
V	Operating voltage	[V]

Greeks letters

η	Overpotential	[Ω m^2]
δ	Thickness	[m]
ρ	Specific ohmic resistance	[Ω m]
φ	Potential	[V]

Subscripts

A	Anode
Act	Activation
C	Cathode
Conc	Concentration
Ohm	Ohmic

สถาบันวิทยบริการ
จุฬาลงกรณ์มหาวิทยาลัย

CHAPTER I
INTRODUCTION

1.1 Motivation of the thesis

Electricity is a critical component for most human activities. It is an important energy source in industrial production and provides essential services to support our standard of living. It should not be surprising therefore, that the levels of household and business activity in the regional economy are the dominant determinants of electricity demand both now and in the future. As a result, APEC Sector Energy Demand Outlook (2000-2020) produced by the Asia Pacific Energy Research Centre as shown in Table 1.1 indicates that the electricity demand will grow at the fastest rate through to 2020.

Table 1.1 APEC sectored energy demand outlook from 2000 to 2020 (Asia Pacific Energy Research Centre, 2002)

	Absoluted Level (Unit:Mtoe)					Annual 1999 - 2010	Average 2010 - 2020	Growth 1999 - 2020
	1999	2005	2010	2015	2020			
Electricity	635.1	762.2	899.9	1050.3	1218.8	3.2%	3.1%	3.2%
Industry	1325	1545	1730.9	1932.3	2152.7	2.5%	2.2%	2.3%
Transport	1035.6	1216	1401.1	1606	1823.9	2.8%	2.7%	2.7%
Commercial	359.3	408.8	459.7	516.2	597.5	2.3%	2.7%	2.5%
Residential	912.3	976	1041.8	117.6	1209.5	1.2%	1.5%	1.4%
Other	127.8	141	153.4	166.8	182	1.7%	1.7%	1.7%

However, electricity generation at the start of the 21st century is affected more by several factors. Feedstock fuels, conversion processes and operating companies will face international competition in a global marketplace where economic viability has the highest priority. Therefore, the long-term prospects for success will mainly

depend on the availability of technology and fuel, on environmental legislation — including climate protection and public acceptance— and on security of supply.

In the most development of sustainable electricity generation, fuel-cell technology is always an interesting alternative currently undergoing a dramatic growth. This new process has been often perceived as being part of the future solution to the 'energy crisis', providing “clean” electricity with virtually no emissions. The development of fuel cells is considered to be an integral part of a sustainable ‘hydrogen economy’, in which hydrogen gas is produced from renewable sources of energy, and which offers the possibility of abundant energy with negligible emissions (Dunn, 2002, Conte *et al*., 2001). Indeed when fuel cells are supplied with pure hydrogen, the only by-product is water vapor and thus is clearly attractive from an environmental standpoint. However, hydrogen does not occur naturally in significant quantities and therefore has to be produced, usually by the reformation of hydrocarbons or electrolyzed from water. Currently fuel cells are nearly always fuelled by natural gas, or by hydrogen produced from natural gas, and thus have some impacts on the environment (Watkiss and Hill, 2002). However, when compared with other technologies, these are still projected to be very small fraction of emissions. As a result, the actual emissions of fuel cells fall well below any current standard of emissions. In general, they will emit less than 1 ppm of NOx, 4 ppm of CO, and 1 ppm of reactive organic gases only, while the standards are an order of magnitude greater for NOx, two orders of magnitude greater for reactive organic gases, and several orders of magnitude larger for CO (Mendoza, 2002).

Furthermore, one of the important characteristics of fuel cell systems is that their efficiency is nearly unaffected by size. This means smaller and relatively higher efficient power plants, when compared on conventional turbine-power plants less than 40% at its maximum efficiency, can be developed until being achievable 45-60% electrical efficiency for single cycle and 90% for total efficiency when the heat recovery is combined (Badwal and Foger, 1996). Therefore, fuel cell technology is very promising for applying in the distributed or centralized power generation industries.

Although there are a variety of fuel cells classified by the type of electrolyte used in the cell, solid oxide fuel cells (SOFCs) have still become a promising option for stationary electricity generation that fits well into the governments' energy plan due to the attractive positive features of their solid-state components including solid-state electrolyte, electrode, and cell interconnects. This means that they have no liquid components with their attendant material corrosion and electrolyte management problems. The SOFCs can also be manufactured in any manner of configurations and operate at high temperature (>800 ^{o}C), having some benefits to be an effective source of by-product heat which can be used for co-generation. Besides, another one of the main attractions of SOFCs over other fuel cells is their ability to handle more convenient hydrocarbon fuels, while other types of fuel cell have to rely on a clean supply of hydrogen for their operation. Because of their high temperature operation, there is the opportunity to reform hydrocarbons within the system either indirectly in a discrete reformer or directly on the anode of the cell, thus offering higher efficiency. In addition, the use of expensive anode material is less required.

Even though the SOFCs in general are very efficient and promising technology for the distributed or centralized power generation industries, a number of researches have been carried out in many directions with a major aim to improve performance of these fuel cells and their systems. Among several procedures for improving fuel cell performance, the use of multiple fuel cell stacks in series concept in which the operating voltage is allowed to vary stack by stack is another interesting approach. Since arranging fuel cell stacks in series still offers several advantages over conventional fuel cell configurations in which multiple stacks are typically arranged in parallel. Stacks networked in series allow the system to operate close to reversible voltages, thus increasing the system efficiency. Higher total reactant utilizations can be achieved by stacks networked in series. Placing stacks in series also allows reactant streams to be conditioned at different stages of utilization. Between stacks, heat can be consumed or removed by heat exchanging which improves the thermal balance of the system. The composition of streams can be adjusted between stacks by mixing exhaust streams or by injecting reactant streams (George and Smith, 2000). However, until now only a few works have focused on the potential benefits of this approach.

Additionally, given the same initial feed streams, the flow rate of reactants through stacks networked in series is much larger than the flow rate of reactants through stacks in conventional configurations. Since conventional fuel cell configurations divide the initial feed streams among many stacks arranged in parallel. While, the initial feed streams in arranging fuel cell stacks in series are not divided, but fed directly into the first of a series of many stacks. Perhaps the greatest disadvantage of is that this increased flow rate creates larger pressure drops.

Therefore, in this research, the comparative study on the operation in conventional SOFC configurations in which multiple stacks are typically arranged in parallel and the alternative ones in which stacks are networked in series is investigated by using MATLAB programming and simulation in order to judge whether SOFC with stacks arranged in series carry out the feasibility analysis of SOFC and propose the best configuration of stack arrangement that provides optimal electrical power without a reduction of electrical efficiency. Additionally, the effect of the generated in-stack pressure drop, number of stacks and compressor configuration on the obtained performance for both conventional and alternative configurations was determined.

1.2 Objective of the work

1. To compare the results of obtained electrical power and efficiency between conventional SOFC configurations in which multiple stacks are typically arranged in parallel and the alternative ones in which stacks are networked in series assuming that the effect of pressure drop is negligible.
2. To study the influence of the generated in-stack pressure drop on attained electrical power and efficiency for both conventional and alternative configurations.
3. To investigate the feasibility of the use of SOFC configuration with stacks arranged in series.

CHAPTER II
THEORY

2.1 Basics of fuel cells

In principle, a fuel cell, which is an electrochemical device, operates like a battery. However, unlike a battery, a fuel cell does not run down or require recharging. It will produce energy in the form of electricity and heat as long as fuel is supplied. The basic physical structure of a fuel cell consists of two electrodes sandwiched around an electrolyte. A schematic representation of a fuel cell with the reactant/product gases and the ion conduction flow directions through the cell is shown in Fig. 2.1.

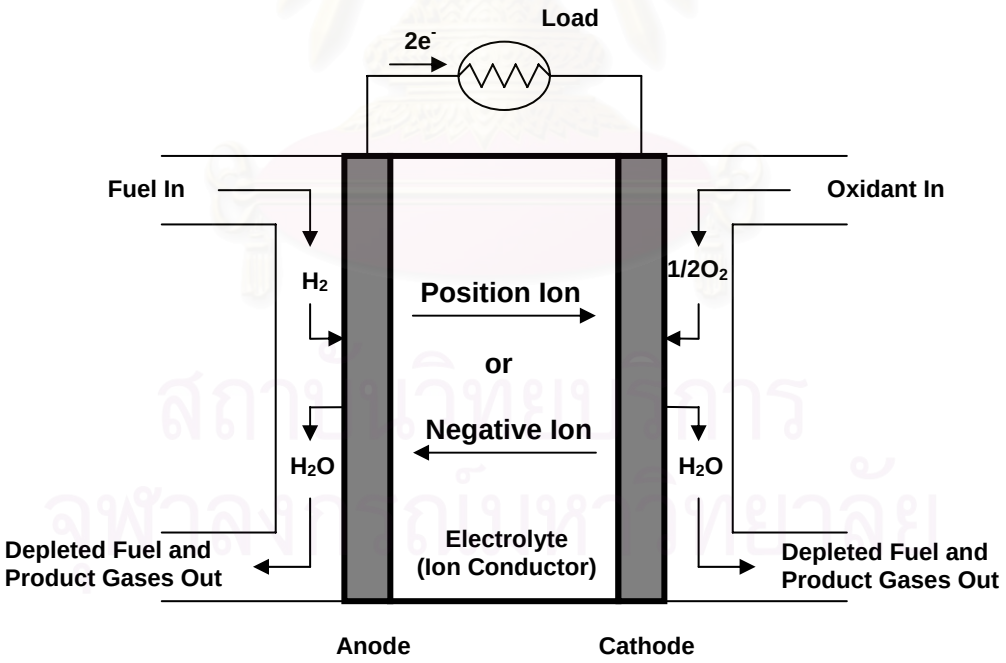

Fig. 2.1 Schematic diagram of an individual fuel cell (Fuel cell handbook, 5th Edition, 2000)

In a typical fuel cell, gaseous fuels are fed continuously to the anode (negative electrode) compartment and an oxidant (i.e., oxygen from air) is fed continuously to the cathode (positive electrode) compartment; the electrochemical reactions take place at the electrodes to produce an electric current. Note that the ion species and its transport direction can differ, influencing the site of water production/removal, and a system impact. The ion can be either a positive or a negative ion, meaning that the ion carries either a positive or negative charge (surplus or deficit of electrons). The fuel or oxidant gases flow past the surface of the anode or cathode opposite the electrolyte and generate electrical energy by the electrochemical oxidation of fuel, usually hydrogen, and the electrochemical reduction of the oxidant, usually oxygen.

Appleby and Foulkes (1989) have noted that in theory, any substance capable of chemical oxidation that can be supplied continuously (as a fluid) can be burned galvanically as the fuel at the anode of a fuel cell. Similarly, the oxidant can be any fluid that can be reduced at a sufficient rate. Gaseous hydrogen has become the fuel of choice for most applications, because of its high reactivity when suitable catalysts are used, its ability to be produced from hydrocarbons for terrestrial applications, and its high energy density when stored cryogenically for closed environment applications, such as in space. Similarly, the most common oxidant is gaseous oxygen, which is readily and economically available from air for terrestrial applications, and again easily stored in a closed environment.

Moreover, a variety of fuel cells are in different stages of development. They can be classified by using diverse categories, depending on the combination of type of fuel and oxidant, whether the fuel is processed outside (external reforming) or inside (internal reforming) the fuel cell, the type of electrolyte, the temperature of operation, whether the reactants are fed to the cell by internal or external manifolds, etc. The most common classification of fuel cells is by the type of electrolyte used in the cells and includes:

1) Polymer electrolyte membrane fuel cell (PEMFC)
2) Alkaline fuel cell (AFC),
3) Phosphoric acid fuel cell (PAFC)
4) Molten carbonate fuel cell (MCFC)
5) Solid oxide fuel cell (SOFC)

These fuel cells are listed in the order of approximate operating temperature, ranging from ~80 ^{o}C for PEMFC, ~100 ^{o}C for AFC, ~200 ^{o}C for PAFC, ~650 ^{o}C for MCFC, and ~800-1000 ^{o}C for SOFC. The operating temperature and useful life of a fuel cell dictate the physicochemical and thermomechanical properties of materials used in the cell components (i.e., electrodes, electrolyte, interconnect, current collector, etc.). Aqueous electrolytes are limited to temperatures of about 200 ^{o}C or lower because of their high water vapor pressure and/or rapid degradation at higher temperatures. The operating temperature also plays an important role in dictating the type of fuel that can be used in a fuel cell. The low-temperature fuel cells with aqueous electrolytes are, in most practical applications, restricted to hydrogen as a fuel. In high-temperature fuel cells, CO and even CH_4 can be used because of the inherently rapid electrode kinetics and the lesser need for high catalytic activity at high temperature. Aside from differences mentioned above, Major further ones between the various cells are shown in Table 2.1.

สถาบันวิทยบริการ
จุฬาลงกรณ์มหาวิทยาลัย

Table 2.1 Summary of major differences of the fuel cell types (Fuel cell handbook, 5th Edition, 2000)

	PEFC	AFC	PAFC	MCFC	SOFC
Electrolyst	Ion Exchange Membranes	Mobilized or Immobilized Potassium Hydroxide	Immobilized Liquid Phosphoric Acid	Immobilized Liquid Molten Carbonate	Ceramic
Operating Temperature	80 ^{o}C	65-220 ^{o}C	205 ^{o}C	650 ^{o}C	800-1000 ^{o}C
Charge Carrier	H^+	OH^-	H^+	CO_3^{2-}	O^{2-}
External Reformer for CH_4	Yes	Yes	Yes	No	No
Prime Cell Components	Carbon-based	Carbon-based	Graphite-based	Stainless-based	Ceramic
Catalyst Product	Platinum	Platinum	Platinum	Nickel	Perovskites
Water Management	Evaporative	Evaporative	Evaporative	Gaseous Product	Gaseous Product
Product Heat Management	Process gas + Independent Cooling Medium	Process gas + Electrolyte Calculation	Process gas + Independent Cooling Medium	Internal Reforming + Process gas	Internal Reforming + Process gas

สถาบันวิทยบริการ
จุฬาลงกรณ์มหาวิทยาลัย

2.2 Fuel cell performance

The purpose of this section is to provide the framework to understand the chemical and thermodynamic operation of fuel cells, i.e., how operating conditions affect the performance of fuel cells. The impact of variables, such as temperature, pressure, and gas constituents, on fuel cell performance needs to be assessed to predict how the cells interact with the power plant system supporting it.

2.2.1 Ideal performance

The electrochemical reaction is occurred by the reaction between fuel and oxidizing agent. The electromotive force (*EMF* or E^0) is theoretical cell voltage. The EMF is calculated from:

$$E^0 = \frac{-\Delta G^0}{nF} \tag{2.1}$$

where, ΔG^0 is Gibb's free energy for standard state conditions (25°C or 298K and 1 atm). *n* is number of electrons passing around the circuit per mole of fuel. *F* is Faraday's constant which always equal to 96485.34 C/mol.

From the general cell reaction in gas phase,

$$\alpha A + \beta B \leftrightarrow cC + \delta D \tag{2.2}$$

The free energy change can be expressed by the equation:

$$\Delta G = \Delta G^0 + RT \ln \frac{p_C^c \; p_D^\delta}{p_A^\alpha \; p_B^\beta} \tag{2.3}$$

When Equations (2.1) is substituted in Equation (2.3),

$$E = E^0 + \frac{RT}{nF} \ln \frac{p_A^\alpha \; p_B^\beta}{p_C^c \; p_D^\delta} \tag{2.4}$$

or

$$E = E^0 + \frac{RT}{nF} \ln \frac{\Pi [reactant \;\; activity]}{\Pi [product \;\; activity]} \tag{2.5}$$

which is the general form of the Nernst equation. For the overall cell reaction, the cell potential increases with an increase in the activity (partial pressure) of reactants and a decrease in the activity of products. Changes in temperature also influence the reversible cell potential, and the dependence of potential on temperature varies with

the cell reaction. The Nernst equations for reaction of hydrogen oxidation, as well as for CO and CH_4 reacting with O_2, that can occur in various fuel cells.

The ideal standard potential of an H_2/O_2 fuel cell (E^0) is 1.229 V with liquid water product and 1.18 for water with gaseous product. This value is shown in numerous chemistry texts (Atkins, 1986) as the oxidation potential of H_2. The potential also can be expressed as a change in Gibbs free energy for the reaction of hydrogen and oxygen. As a result, the change in Gibbs free energy increases as cell temperature decreases and that the ideal potential of a cell, is proportional to the change in the standard Gibbs free energy.

2.2.2 Actual performance

Useful work (electrical energy) is obtained from a fuel cell only when a reasonable current drawn, but the actual cell potential is decreased from its equilibrium potential because irreversible losses as shown in Fig. 2.2. Several sources contribute to irreversible practical fuel cell. The losses, which are often called polarization, overpotential, or overvoltage (η), originate primarily from three sources: 1) Activation polarization (η_{act}), 2) Ohmic polarization (η_{ohm}), and 3) concentration polarization (η_{conc}). These losses result in a operating voltage (V) for a fuel cell that is less than its ideal potential, E^0.

.

$$V = E - \eta_{act} - \eta_{ohm} - \eta_{conc} \quad (2.6)$$

สถาบันวิทยบริการ
จุฬาลงกรณ์มหาวิทยาลัย

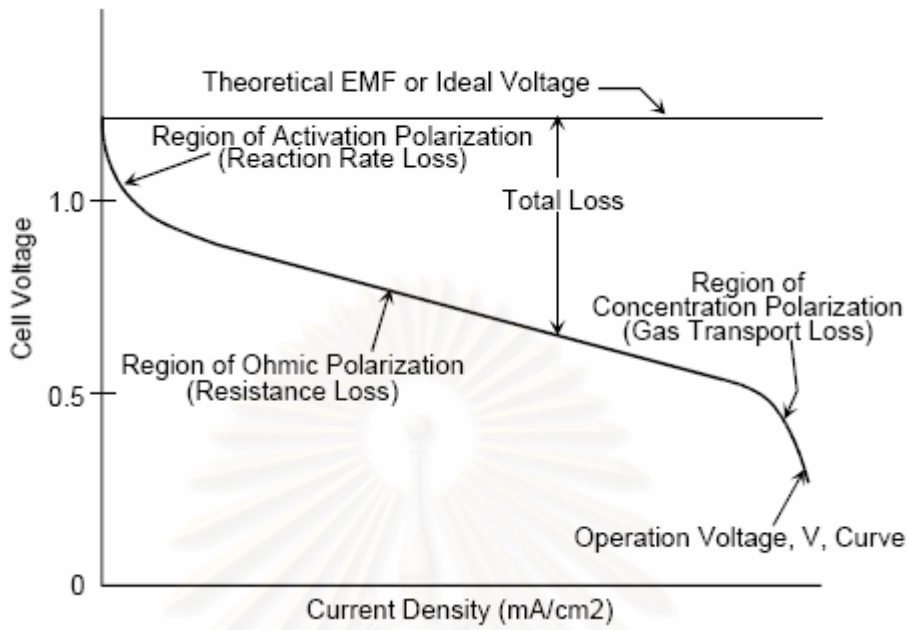

Fig. 2.2 Ideal and actual fuel cell voltage/current characteristic (Fuel cell handbook, 5th Edition, 2000)

The activation polarization loss is dominant at low current density. At this point, electronic barriers have to be overcome prior to current and ion flow. Activation losses show some increase as current increases. Ohmic polarization (loss) varies directly with current, increasing over the whole range of current because cell resistance remains essentially constant. Gas transport losses occur over the entire range of current density, but these losses become prominent at high limiting currents where it becomes difficult to provide enough reactant flow to the cell reaction sites.

Activation overpotential (η_{Act})

Activation polarization is present when the rate of an electrochemical reaction at an electrode surface is controlled by sluggish electrode kinetics. In other words, activation polarization is directly related to the rates of electrochemical reactions. There is a close similarity between electrochemical and chemical

reactions in that both involve an activation barrier that must be overcome by the reacting species.

The electrode reaction rate at high temperatures is fast, leading to low activation polarization as commonly deserved in SOFC.

Ohmic overpotential (η_{Ohm})

Ohmic losses occur because of resistance to the flow of ions in the electrolyte and resistance to flow of electrons through the electrode materials. The dominant ohmic losses, through the electrolyte, are reduced by decreasing the electrode separation and enhancing the ionic conductivity of the electrolyte. Because both the electrolyte and fuel cell electrodes obey Ohm's law, the ohmic losses can be expressed by the equation

$$\eta_{Ohm} = iR \tag{2.7}$$

where i is the current flowing through the cell, and R is the total cell resistance, which includes electronic, ionic, and contact resistance.

Concentration overpotential (η_{Conc})

As a reactant is consumed at the electrode by electrochemical reaction, there is a loss of potential due to the inability of the surrounding material to maintain the initial concentration of the bulk fluid. That is, a concentration gradient is formed. Several processes may contribute to concentration polarization: slow diffusion in the gas phase in the electrode pores, solution/dissolution of reactants/products into/out of the electrolyte, or diffusion of reactants/products through the electrolyte to/from the electrochemical reaction site. At practical current densities, slow transport of reactants/products to/from the electrochemical reaction site is a major contributor to concentration polarization. This means that concentration polarization becomes an important loss at high current densities and small fuel concentrations.

2.3 Solid oxide fuel cells

Solid oxide fuel cells (SOFCs) have grown in recognition as a viable high temperature fuel cell technology. There is no liquid electrolyte with its attendant material corrosion and electrolyte management problems. The operating temperature of >800 ^{o}C allows internal reforming, promotes rapid kinetics with nonprecious materials, and produces high quality byproduct heat for cogeneration or for use in a bottoming cycle, similar to the MCFC. The high temperature of the SOFC, however, places stringent requirements on its materials. The development of suitable low cost materials and the low cost fabrication of ceramic structures are presently the key technical challenges facing SOFCs (Mihn, 1993).

The solid state character of all SOFC components means that, in principle, there is no restriction on the cell configuration. Instead, it is possible to shape the cell according to criteria such as overcoming design or application issues. Cells are being developed in two different configurations, as shown in Fig. 2.3. One of these approaches, the tubular cell, has undergone development at Siemens Westinghouse Corporation and its predecessor since the late 1950s. During recent years, Siemens Westinghouse developed the tubular concept to the status where it is now being demonstrated at user sites in a complete, operating fuel cell power unit of nominal 100 kW (net AC) capacities.

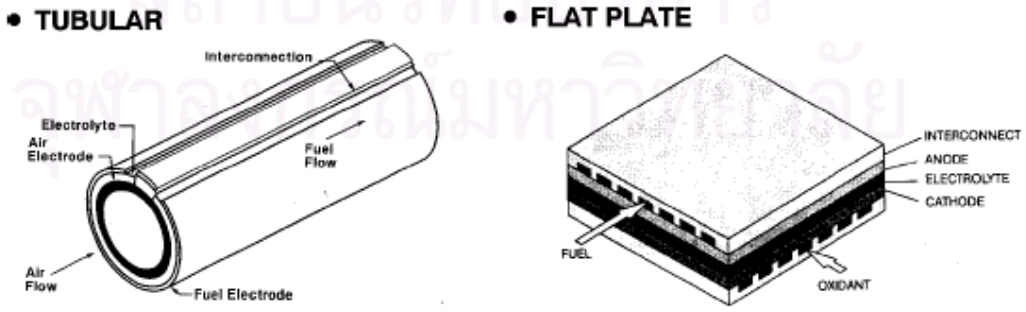

Fig. 2.3 Solid oxide fuel cell designs at the cathode (Fuel cell handbook, 5th Edition, 2000)

The electrochemical reactions (Fig. 2.4) occurring in SOFCs utilizing H_2 and O_2 are based on Equations (2.8) and (2.9):

$$H_2 + O^{2-} \leftrightarrow H_2O + 2e^- \quad (2.8)$$

at the anode, and

$$\frac{1}{2}O_2 + 2e^- \leftrightarrow O^{2-} \quad (2.9)$$

at the cathode. The overall cell reaction is

$$H_2 + \frac{1}{2}O_2 \leftrightarrow H_2O \quad (2.10)$$

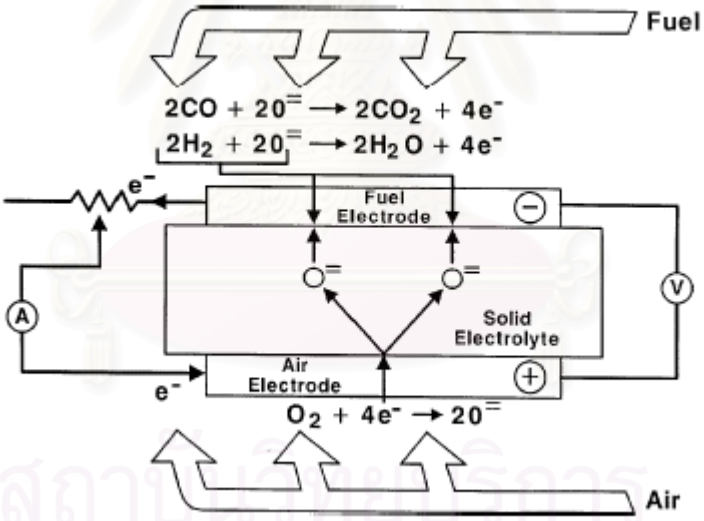

Fig. 2.4 Solid oxide fuel cell operating principle (Courtesy of Siemens Westinghouse, 2002).

The corresponding Nernst equation, Equation (2.11), for the reaction in Equation (2.10) is

$$E = E^0 + \frac{RT}{2F}\ln\frac{p_{H_2}\, p_{O_2}^{1/2}}{p_{H_2O}} \qquad (2.11)$$

Carbon monoxide (CO) and hydrocarbons such as methane (CH_4) can be used as fuels in SOFCs. It is feasible that the water gas shift involving CO ($CO + H_2O \rightarrow H_2 + CO_2$) and the steam reforming of CH_4 ($CH_4 + H_2O \rightarrow 3H_2 + CO$) occur at the high temperature environment of SOFCs to produce H_2 that is easily oxidized at the anode. The direct oxidation of CO in fuel cells also is well established. It appears that the reforming of CH_4 to hydrogen predominates in the present SOFCs. SOFC designs for the direct oxidation of CH_4 have not been thoroughly investigated in SOFCs in the past (Etsell and Flengas, 1971, Isenberg, 1977) nor lately (no significant work was found). For reasons of simplicity in this handbook, the reaction of CO is considered as a water gas shift rather than an oxidation. Similarly, the favored reaction of H_2 production from steam reforming is retained. Hydrogen produced by the water gas shift and the reforming of methane is included in the amount of hydrogen subject to reaction in Equations (2.8), (2.10), and (2.11).

Furthermore, Table 2.2, shown below, provides a brief description of the materials currently used in the various cell components of the more developed tubular SOFC, and those that were considered earlier. Because of the high operating temperatures of present SOFCs (approximately 1000 ^oC), the materials used in the cell components are limited by chemical stability in oxidizing and reducing environments, chemical stability of contacting materials, conductivity, and thermomechanical compatibility. These limitations have prompted investigations of developing cells with compositions of oxide and metals that operate at intermediate temperatures in the range of 600-800 ^oC

Table 2.2 Evolution of cell component technology for solid oxide fuel cells (Fuel cell handbook, 5th Edition, 2000)

	ca. 1965	ca.1975	Current Status
Anode	- Porous Pt	- Ni/ZrO_2 cerment[a]	- Ni/ZrO_2 cerment[a] - Deposit slurry, EVD Fixed[c] - 12.5 x 10^{-6}cm/cm ^oC - ~150 μm thickness - 20-40% porosity
Cathode	- Porous Pt	- Stabilized ZrO_2 impregnated with praesodymium oxide and covered with SnO doped In_2O_3	- Doped lanthanum manganite - Extrusion, sintering - ~2 μm thickness - 11 x 10^{-6}cm/cm ^oC expansion from room temperature to 1000 ^oC - 30-40% porosity
Electrolyte	- Yttria stabilized ZrO_2 - 0.5 mm thickness	- Yttria stabilized ZrO_2	- Yttria stabilized ZrO_2 (8 mol%Y_2O_3) - EVD[d] - 10.5 x 10^{-6} cm/cm ^oC expansion from room temperature to 1000 ^oC - 30-40 μm thickness
Cell Interconnect	- Pt	- Mn doped cobalt chromite	- Doped lanthanum chromite - Plasma spray - 10 x 10^{-6} cm/cm ^oC - ~100 μm thickness

a - Specifications for Siemens Westinghouse SOFC.

b - Y_2O_3 stabilized ZrO_2

c - Fixed EVD means additional ZrO_2 is grown by EVD to fix (attach) the nickel anode to the electrolyte. This process is expected to be replaced by anode sintering.

d - EVD = electrochemical vapor deposition

CHAPTER III
LITERATURE REVIEWS

Fuel cells are promising power generation systems of high efficiency because they can convert the free energy change of a chemical reaction directly into electrical energy. Among different kinds of fuel cells, solid oxide fuel cells (SOFCs) offer significant advantages for the highest efficient electrochemical energy conversion for stationary applications Due to their high operating temperatures (between 800 and 1000 ^{o}C), a wide variety of fuels and effective source of by-product heat which can be used for co-generation can be processed. Therefore, a number of researches have been carried out in many directions with a major aim to improve performance of these fuel cells and their systems. Among several procedures for improving fuel cell performance, the use of multistage configuration with a set of serially connected fuel cell stacks in which the operating voltage is allowed to vary in each stack is another interesting approach. However, until now only a few works have focused on the potential benefits of this approach. Moreover, large pressure drops and serious mechanical problems from the increase of fuel, fed directly into the first of a series of many stacks, are still major constraints for further development of this approach in the future.

3.1 A wide variety of fuels for solid oxide fuel cells

Since natural gas is a relatively cheap and commonly available fuel. Its main component is methane. Therefore, nearly all of the state of the art SOFC-systems is designed for operation on natural gas, which has to be converted into a mixture of hydrogen, carbon monoxide, water and carbon dioxide by steam reforming, partial oxidation or autothermal reforming to avoid cracking and carbon-deposition at the anode (Weber *et al.*, 2002). The reforming of methane by steam or CO_2, i.e.

$$CH_4 + H_2O \leftrightarrow CO + 3H_2 \quad (3.1)$$

$$CH_4 + CO_2 \leftrightarrow 2CO + 2H_2 \quad (3.2)$$

yielding H_2 and CO, has received renewed interests today because of the possibility of enhancing natural gas valorization Bradford and Vannice (1999) and Nielsen (1983). The reforming process can be considered as an inexpensive way of H_2 production but this is also the conventional industrial process for the production of synthesis gas ($CO + H_2$), which then can be used in the Fisher–Tropsch synthesis industry to produce valuable chemicals. Moreover, H_2, CO or H_2 + CO mixtures produced by the reforming process can be used as efficient fuels for high temperature SOFCs to produce electricity (Stoukides, 2000). Methane fuelled SOFC plants for electrical energy production often involve an external reformer, where methane is converted to CO and H_2 before these gases are supplied to the fuel cell compartment of the plant.

Hirschenhofer *et. al.* (2000) indicated that the operating temperature also plays an important role in dictating the type of fuel that can be used in a fuel cell. The low-temperature fuel cells with aqueous electrolytes are, in most practical applications, restricted to hydrogen as a fuel. In high-temperature fuel cells, such as SOFC is their ability to use CO as a fuel because of the inherently rapid electrode kinetics and the lesser need for high catalytic activity at high temperature. However, the anodic oxidation of CO in an operating SOFC is slow compared to the anodic oxidation of H_2; thus, the direct oxidation of CO is not favored. Moreover, the water gas shift reaction (Eq. 3.3) reaches equilibrium rapidly at temperatures as low as 650 ^oC to produce H_2.

$$CO + H_2O \leftrightarrow H_2 + CO_2 \quad (3.3)$$

As H_2 is consumed, the reaction is driven to the right because both H_2O and CO_2 are produced in equal quantities in the anodic reaction. Because of the shift reaction providing the necessary additional H_2 that is oxidized at the anode, the high fuel utilization is possible.

3.2 Several approaches for performance improvement of solid oxide fuel cells

Solid oxide fuel cells are energy conversion devices that produce electricity via the electrochemically combining reactions of fuel and oxidant gases across an ionic-conducting ceramic. The SOFCs have attracted special interests as a method of future electric power generation because of high efficiency and pollution-free operation. Furthermore, they are made entirely of solid materials for high reliability. The high temperature (800–1000^{o}C) exhaust heat obtained simultaneously with power generation is used in fuel reforming, bottoming power generation, and the regenerative heating of fuel and air, as a result of which the total power generation efficiency of the entire cycle is high. It has been demonstrated by simulation technique that SOFC can achieve 50% net electrical efficiencies and have already been considered feasible for integration with multi-MW gas turbine engines to achieve considerably high electrical efficiency (Massardo and Lubelli, 2000). Thus, these different forms of SOFC implementations are predicted to be widely available for use in society in the near future.

Several articles have been devoted to the study of SOFC–GT combined power co-generation systems. Most of these studies have considered a natural gas-fueled SOFC–GT system with steam reforming and heat recuperation (HR, air preheating). Siemens-Westinghouse Power Corporation developed the first advanced power system, which integrates a SOFC stack with the gas turbine engines. The pressurized (3 atm) system generates 220 kW of electrical power at a net electrical efficiency of 55% (Hirschenhofer *et al*., 2000). Furthermore, Palsson *et al.* (2000) developed a two dimensional, steady-state SOFC model and proposed a combined system featuring external pre-reforming and recirculation of anode gases. They reported that the maximum efficiency of 65% (LHV) was obtained at a pressure ratio of 2. Increasing the turbine inlet temperature (TIT) does not lead to an improvement of efficiency or specific power because at higher TIT, more fuel is consumed in the gas turbine, decreasing the fuel flow to the SOFC unit. Tanaka *et al.* (2000) have designed and evaluated a SOFC–GT combined system based on system performance and cost/energy pay-back times. They mentioned the similar result for the influence of

TIT on overall efficiency. A small GT power output to net output is desirable for overall performance. In fact, the GT output from a combined SOFC–GT system is about one-third of the total output (Palsson *et al.*, 2000). Despite various proposals for system configurations and prototype tests during the last several years, SOFC-GT systems have only been developed for kW-class power generations (Veyo *et al.*, 2002, Litzinger *et al.*, 2005). However, as indicated in the Vision 21 Technology Roadmap announced by the Department of Energy, USA in 1999, a SOFC-GT system will ultimately be developed for commercial entry into multi-MW distributed generation applications. To apply a SOFC-GT hybrid system to large power generations, the amount of power generated by both the SOFC and gas turbine must be increased. In general, increasing the number of unit cells and/or sub-stack modules can raise the SOFC power. With the exception of its size, there are no dramatic changes in the SOFC configuration with an increased generated power.

Besides, in present development of SOFCs, it is also focused on lowering the operating temperature below 800◦C. The advantages of a reduced-temperature operation for SOFCs include wider material choice, better long-term performance, system compactness, and potentially reduced fuel cell costs (Mihn and Takahashi, 1995, Matsuzaki and Yasuda, 1998, Tu *et al.*, 1999). However, it does increase the electrolyte resistivity and decrease the ionic conductivity. This can be overcome by lowering the electrolyte resistance either by using a thin Y_2O_3 stabilized ZrO_2 electrolyte or by using higher ionic conductive materials. Ishihara *et al.* (1994) have investigated that a recent low temperature SOFC with a lanthanum gallate electrolyte that can be operated from about 600^{o}C has shown superior power generation characteristics, thereby expanding the operating temperature range of SOFCs. Since the power generation efficiency of a fuel cell is higher than that of a gas turbine. Thus, expansion of the operating temperature range of SOFC is promising for increased system power generation efficiency. Moreover, Yoon *et al.* (2002, 2003, 2004) reported a new method of improving electrode performance by coating thin films of YSZ or samaria-doped ceria (SDC) within the pores of electrode by a sol–gel coating technique. This process is a very simple and cost-effective way that proves to be less restricted by geometric limitations (e.g. shape, size, etc.)

3.3 An interesting approach: The concept of multiple fuel cell stacks in series

Among several procedures for improving fuel cell performance, the use of multistage configuration with serially connected fuel cell stacks whose operating voltage is allowed to vary stack by stack is another interesting approach. By connecting the stacks in series, more homogenous current distribution over the cell surface can be achieved, resulting in lower polarization losses (Standaert *et al.*, 1998).

George *et al.* (1998) stated that the United States Department of Energy (DOE) has investigated ways to achieve high power generation efficiency of 80% and has proposed a multi-staged fuel cell system with five serial stages of fuel cells in order to reduce the regenerative heat for fuel and air, and to extend the operating temperature range of fuel cells. Moreover, Senn and Poulikakos (2005) investigated the performances of Polymer electrolyte membrane fuel cells (PEMFC) divided into many stages of equal stage size. It was demonstrated that the non-uniform cell potential operation allows for enhanced maximum electric cell power densities compared to the traditional concept involving a uniform cell potential distribution. The improvement of maximum power density within 6.5% was reported. The multistage operation of the molten carbonate fuel cell (MCFC) was studied (Au *et al.*, 2003). When both anode and cathode flows in series, the improved performance is about 0.6%. Additionally, the anode flow in series while keeping the cathode flow parallel show improved performance up to 0.3%.

For MCFC, it is shown that an improvement in electric efficiency of about 1% can be achieved by splitting the cell area into 2 segments (Standaert, 1998). This conclusion was based on both analytical mathematical modeling and simplified flowsheet calculations. Liebhafsky and Cairns (1968) and Selimovic and Palsson (2002) both have also considered the use of multistage operation, but then for SOFC. They showed that an improvement in power output of about 5% point can be obtained for their systems.

CHAPTER IV
MODEL DEVELOPMENT

4.1 Mathematical model of SOFC

A mathematical model of SOFC presented here, examining electrochemical and flow effects, includes seven different domains corresponding to the following components: cathode interconnect, air channel, cathode, electrolyte, anode, fuel channel, and anode interconnect. The chemical reactions are inside the electrodes. Water vapor is produced in the anode, and oxygen ions produced in the air electrode (cathode). At high temperature, no condensation of water in the anode is expected. It is assumed that the SOFC stacks are operated under steady state and isothermal. In this case, operating temperature is maintained to keep at 1173 K (900^{o}C)

This model is developed for a SOFC in the planar and co-flow configuration. It has been reported that the planar-type design of SOFC has the potential to offer higher power density than the tubular design (Khaleel *et al.*, 2004). Due to its compactness, it can be stacked in resemblance to polymer electrolyte membrane fuel cells (PEMFCs) to satisfy the power requirement of an application (Recknagle *et al.*, 2003). Higher power density of planar SOFC is due to the shorter current paths resulting in low ohmic overpotential. Moreover, planar SOFC is simple to fabricate and can be manufactured into various configurations (Yakabe *et al.*, 2001). However, the problems associated with the development and commercialization of planar SOFC are requirement of high temperature gas seals, internal compressive stresses in cell components. In this study, it is assumed that the outlet pressure from cell channels is always equal to atmosphere which is typical pressure for several previous literatures. In addition, the cell channels of planar type SOFC also have slimmer cross section than the tubular type SOFC. By this reason, this type SOFC is more possible to encounter influence of generated pressure drop in cell channel whose effect is taken into account in this work. The schematic diagram of a planar type SOFC stack is

illustrated in Fig. 4.1. Furthermore, the typical information is given by Iwata *et al.* (2000) and Pasaogullari and Wang (2003). Fig 4.2 shows the typical SOFC dimensions considered as the basic configuration (Costamagna and Honegger, 1998, Vandersteen *et. al.*, 2004). In single cell, The interconnects are in the form of ribs with the twenty air channels for the air side interconnect and twenty fuel channels for the fuel side interconnect corresponding to location of the rib roots, and the gas channel locations to the rib tips. The stack module is a column of 100 cells (30 cm x 30 cm x 60 cm) connected with interconnects. Thus, one standard stack in this work has the total cell area at 1.2 m^2. In the next section, these stacks will be connected in different configuration in which each stack size is still fixed at given above value.

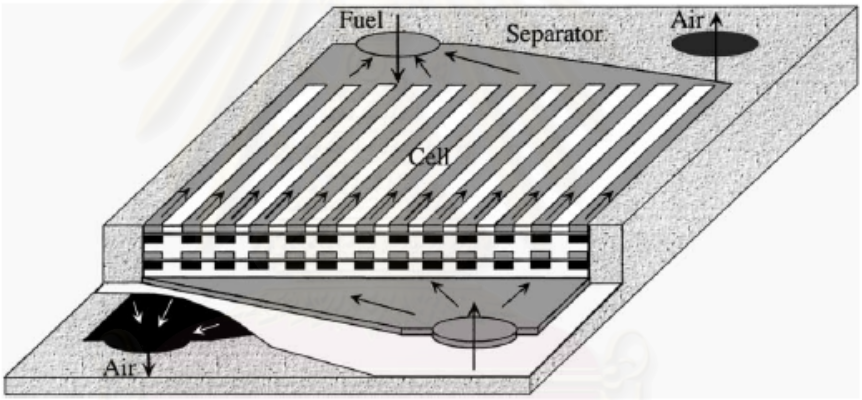

Fig 4.1 The schematic diagram of a planar type SOFC stack with internal manifolds (Yakabe *et. al.*, 2001)

สถาบันวิทยบริการ
จุฬาลงกรณ์มหาวิทยาลัย

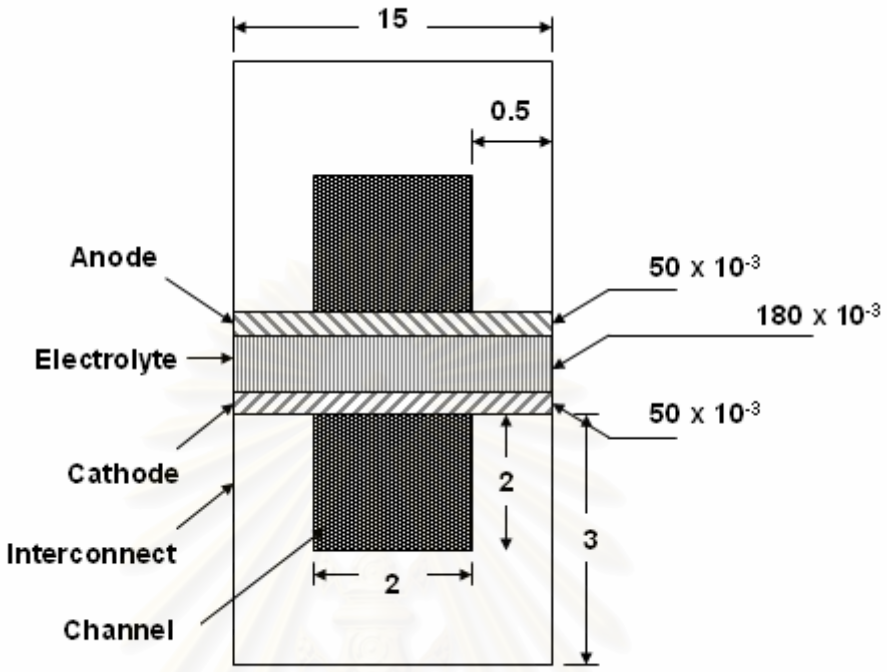

Fig 4.2 The typical SOFC dimensions in unit of millimeters.

The SOFC model can be used with a non-hydrogen fuel which is methane in case of this work, a reformer is generally required to reform the fuel with an oxidant (e.g. steam) to a hydrogen-rich stream before feeding to the SOFC stack The main reactions, whose operating temperature is kept constant at 973 K (700^{o}C), implicated to methane steam reforming and water gas shift reactions in the production of hydrogen from methane and steam as shown in Eq. (3.1) and Eq. (3.3) on which the outlet composition before feeding to the SOFC stack consists of 1.50% CH_4, 12.77% CO, 5.93% CO_2, 62.01% H_2 and 17.79% H_2O. In the SOFC stack, hydrogen can react electrochemically with oxygen only assuming that the CO electro-oxidation in an operating SOFC is slow compared to the H_2 electro-oxidation. Moreover, water gas shift reaction still take place along the stack channel according to be able to reach its equilibrium at temperatures more than 650^{o}C to produce the necessary additional H_2 that is oxidized at the anode.

4.1.1 Electrochemical model

The electrochemical module determines the current density distribution inside the cell. The electrochemical reactions of hydrogen and oxygen take place in this work according to Eq. (4.1) and Eq. (4.2).

Anode: $H_2 + O^{2-} = H_2O + 2e^-$ (4.1)

Cathode: $O_2 + 4e^- = 2O^{2-}$ (4.2)

An electrochemical analysis based on deviations from ideal performance is proposed at each slice. Considering the electrodes to be equipotential surfaces, the ideal or Nernst voltage is defined in Eq (2.5). In practice, the actual SOFC voltage is decreased from its open circuit voltage because of irreversible losses.

Irreversibilities, also known as polarizations or overpotentials, cause voltage losses from the Nernst voltage value and have a negative impact on fuel cell performance. There are three types of overpotentials:

1.) Activation overpotentials, η_{act}.

2.) Ohmic overpotentials, η_{Ohm}.

3.) Concentration overpotentials, η_{conc}.

Multidimensional models previously developed frequently include activation and ohmic losses but not concentration loss as this is one order of magnitude smaller under usual operating conditions. In high temperature fuel cells, the activation overpotential in high temperature fuel cell is less significant. The activation overpotential of electrolyte-supported SOFC occurs in both electrodes, the activation overpotential of the cathode is obviously higher than that of the anode due to its lower exchange current density. The activation overpotential increases steeply at low current density but gradually at higher current density. The activation overpotential can be determined from Butler–Volmer equation which is used to relate the surface

overpotential and the rate of reaction (Newman and Thomas, 2004). Besides, ohmic polarization indicating the electronic and ionic resistance through the electrodes and electrolyte, respectively, is determined by using Ohm's law The total cell resistance is calculated in terms of the resistivity and an equivalent area corresponding to the thickness of the electrodes or electrolyte. The resistivity for the SOFC materials was based on the values reported by Bessette (1995) (see Appendix C).

To simplify the calculations of the SOFC performance, concentration overpotential due to mass transport effect is neglected such overpotential becomes important at low concentration of the reactant gases and high value of current density. This system is not expected to operate in such conditions (actually such phenomena should be taken into account if the CO electrochemical reaction is considered).

4.1.2 Fuel utilization factor and fuel cell efficiency

Fuel utilization factor and fuel cell efficiency are among the most important parameters to evaluate fuel cell performance. The amount of fuel and oxidant consumed in a fuel cell is defined by the fuel utilization, which affect both the fuel cell performance and its efficiency. The definitions and calculation of those parameters are described next.

4.1.2.1 Fuel utilization factor

The fuel utilization factor (U_f) refers to the fraction of the total fuel introduced into a fuel cell that reacts electrochemically (Hirschenhofer, 1998). For SOFC applications, hydrogen and carbon dioxide are considered as fuels. However, from mentioned above, hydrogen can react electrochemically with oxygen and carbon monoxide takes place the water gas shift reaction to produce additional hydrogen only. Therefore, in this case, the fuel utilization factor is defined as 100%, the fuel utilization is determined as:

$$U_f = \frac{H_2 \ consumed}{H_{2,in} + CO_{in}} \quad (4.3)$$

It should be noted here that moles of hydrogen consumed in an SOFC due to electrochemical reactions are related to the current generation according to the Faraday's law (Aguiar, 2002). When hydrogen participates in electrochemical reactions, the amount of hydrogen (n_{H_2}) consumed is determined as,

$$n_{H_2} = \frac{i \cdot A}{2F} \quad (4.4)$$

where i is the current densities produced by hydrogen oxidation reactions. A is the geometrical area of the fuel cell. Typically, fuel utilization factor should be kept as high as possible. Unfortunately, the cell performance decreases dramatically as the fuel utilization factor approaches 100% (Braun, 2002). Therefore, fuel utilization for commercial SOFCs is maintained between 75 and 85% (Suwanwarangkul *et. al.*, 2006).

4.1.2.2 Fuel cell efficiency

Fuel cell efficiency is used to evaluate the capability of converting energy stored in fuel into electrical power. It is typically expressed in terms of thermal efficiencies, which is defined as an amount of useful energy produced relative to the change in stored chemical energy (commonly referred to thermal energy) that is released when a fuel reacts with an oxidant (Hirschenhofer, 1998).

$$\eta_{thermal} = \frac{Pow}{\Delta H_f} \quad (4.5)$$

where Pow and ΔH_f represent electrical power generated by SOFC and enthalpy or thermal energy supplied to a fuel cell, respectively. For an SOFC, ΔH_f using methane to be reformed to a hydrogen-rich stream before feeding to the SOFC stack is determined as:

$$\Delta H_f = F_{CH_4} LHV_{CH_4} \quad (4.6)$$

where LHV_{CH_4} are lower heating values for methane in the unit of J mol^{-1}, *i.e.*, enthalpy of combustion at 298 K assuming that the water product is in the form of steam. F_{CH_4} is the molar flow rates of methane fed into reformer in units of mol s^{-1}.

4.2 Model Validation

In the most model validation, the electrochemical module is able to be validated using experimental data from an experimental setup aimed at the study of the tolerance analysis on SOFC systems (Singh, 2004). The model is used to identify some of the performance characteristics of the experimental results, and the experiments are used to fix some predetermined parameters in the model such as the exchange current density of activation overpotential and ohmic resistance constant of ohmic overpotential. Although this is a common practice, once the model is adjusted to these fixed parameters, the model will be unique to one specific setup. However, for the calculations presented in this research, more general expressions for predicting some predetermined parameters as shown in Appendix C is used and verified following the previous work of Eduardo *et al.* (2005) which is the original reference of electrochemical model development for this work.

4.3 System configuration

In SOFC network analysis, the basic principle of a fuel cell network is staging of the fuel flow path. This is described as having the fuel pass a number of separate or segmented electrical circuits on its way through the fuel cell array (Hirschenhofer, 2000). Fig. 4.3b illustrates how the reactant streams in a fuel cell network flow in series from stack to stack in example of two stacks.

In this way, the partially utilized fuel exhaust stream from one stack becomes the inlet fuel for the next stack. In conventional configuration, the fuel feed is divided into equal streams which flow in parallel through the fuel cell stack (Fig 4.3a). Further, in the figure, the maximum power that could be generated by two different SOFC systems having identical feed stream compositions is compared. Each system converts an amount of fuel into heat and electrical work and the stack area is the same in both cases. For the networked stack, a part of the fuel flow is converted in the first stage at fuel utilization, U_f^*, while the fuel utilization of the second stage is chosen such that the total utilization of the stacks in the same as in the single stage stack. As diagram indicates that it may be possible in the networked stacks in series to transfer charges at rather higher reversible voltages (V_2, V_3) and hence to convert more of free energy directly into electrical energy and less into heat. The low voltage associated with high utilization, which is typical for conventional single stacks, is restricted in the networks to stacks which produce only a portion of total power (second stage in Fig. 3.3b)

สถาบันวิทยบริการ
จุฬาลงกรณ์มหาวิทยาลัย

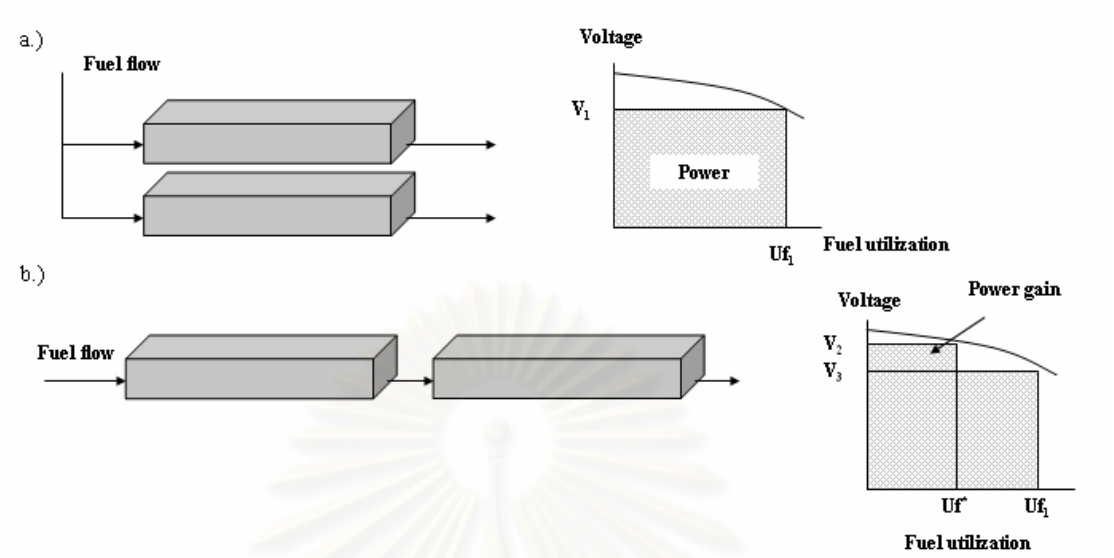

Fig. 4.3 Schematic representation of fuel flow configurations for two stacks in a) parallel b) series

The SOFC system calculations described here were performed using MATLAB, whereas different SOFC systems are modeled as the single reference stack and arranged reference ones in either parallel or series. Firstly, theoretical models, assuming that the effect of pressure drop is negligible, are considered. It is very common assumption in developing SOFC models. However, from earlier chapter, it is obvious that the flow rate of reactants through stacks networked in series is much larger than the flow rate of reactants through stacks in conventional configurations by giving the same initial feed streams. Therefore, particular study in the influence of the generated in-stack pressure drop is unavoidable in order to investigate the practical feasibility of the use of SOFC configuration with stacks arranged in series and estimate the actual net power from obtained electrical power in SOFC minus the power consumption of some installed compressors in compensating the pressure loss to maintain the outlet pressure from cell channels at atmosphere.

In the start of study, it is assumed that the effect of pressure drop is negligible, it is essential to understand obviously in several simple effects in a single reference stack as to find out the suitable operating condition that provides optimal electrical power and efficiency. These ones include some effect of methane feed flow rate into

external reformer, corresponding directly fuel flow rate into fuel cell stacks, and operating voltage of stack. From available optimal operating condition, then, each single stack is taken a connection in either parallel or series. The amount of methane feed flow rate fed into external reformer will depend on a number of connected stacks significantly, that is, the amount of methane feed flow rate fed into external reformer in both parallel and series configurations is equal to available methane feed flow rate in single stack multiplied by a number of connected stacks as to keep up the obtained electrical power and efficiency from multiple stack operation not less than single stack one. In this case, we compare the results of obtained electrical power and efficiency in the same number of stacks between conventional SOFC configurations in which multiple stacks are typically arranged in parallel and the alternative ones in which stacks are networked in series. Effect of the increase of number of stacks for both conventional and alternative configurations is also investigated.

In another case, the study is subjected to influence of the generated in-stack pressure drop of both conventional and alternative configurations mainly. The way to study is similar to the previous case. But, it is different that, in term of the percentage of generated pressure drop, this work considers both anodic and cathodic channels based on outlet pressure at atmosphere for which the required inlet pressure of each stack is dependent on operating voltage and stack configuration significantly. By this reason, it is necessary to compress both fuel and air into these required inlet pressure by using fuel and air compressors. This further installation indicates that a part of obtained electrical power has to be consumed to operate some compressors. In this work, since the heat recovery system (shadowed area in Fig 4.4) is not considered, electrical power is generated from SOFC system only. Thus, the actual net power is equal to obtained electrical power from SOFC system minus power consumption of fuel and air compressors.

This work will investigate on three configurations following multiple stack arrangement in both parallel (Fig 4.4a) and series. Especially in series, arrangement between stacks and compressor is separated possibly into two configurations

including:

1) One compressor installed before SOFC system whose outlet pressure is at atmosphere (Fig. 4.4b).
2) Staged compressors installed with every stacks whose outlet pressure is at atmosphere (Fig 4.4c).

The actual net power of all configurations is determined and compared to propose the best configuration of stack and compressor arrangement that provides optimal electrical power without a reduction of electrical efficiency.

สถาบันวิทยบริการ
จุฬาลงกรณ์มหาวิทยาลัย

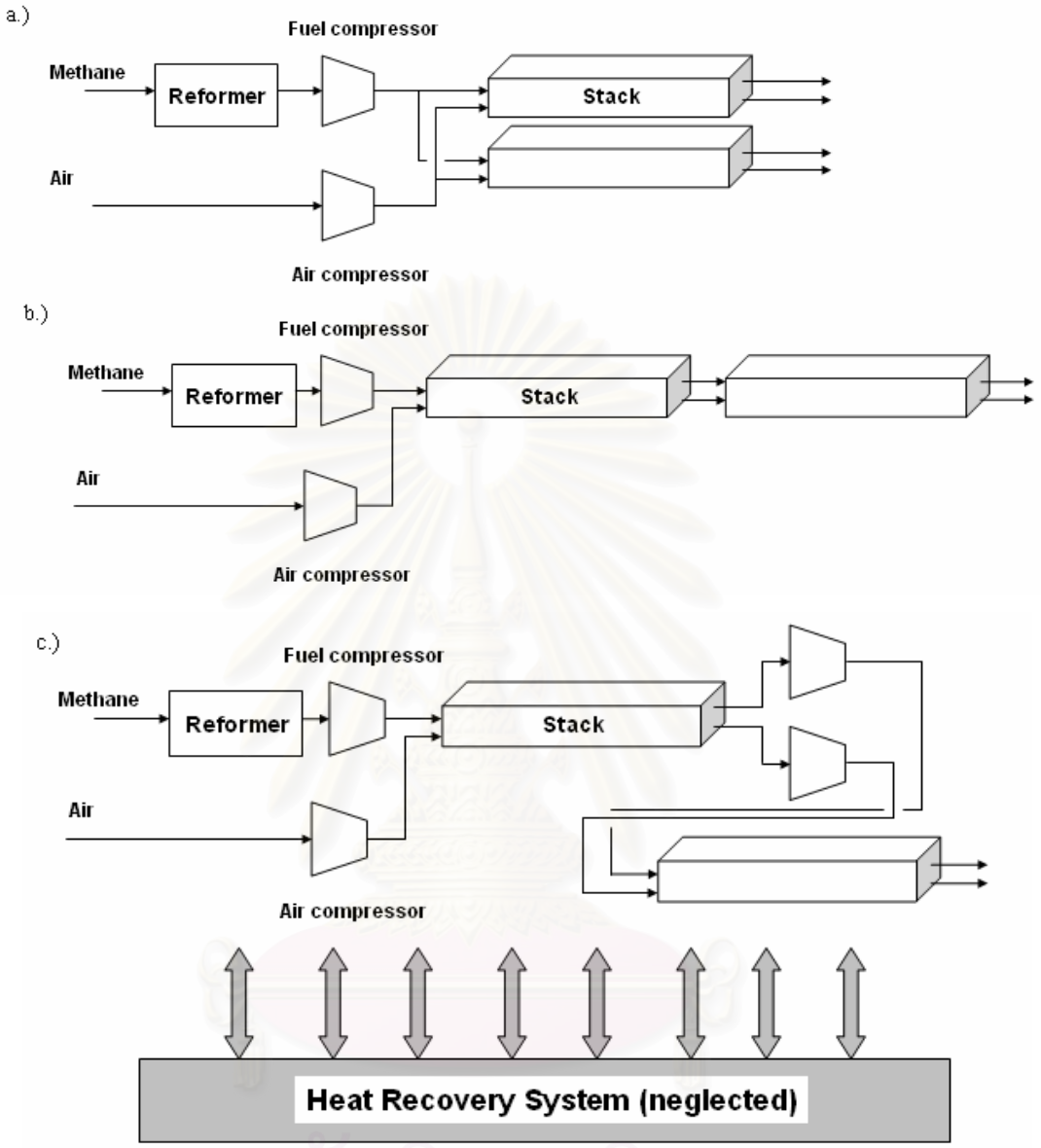

Fig. 4.4 SOFC and compressor configurations for two stacks in a.) parallel with one compressor installed before SOFC system b.) series with one compressor installed before SOFC system c.) series with staged compressors installed with every stacks.

CHAPTER V
RESULTS AND DISCUSSION

Results and discussion of this work is provided in this chapter. The study begins with the model validation by comparing the simulation results with those from the published literature. Then the improvement of the SOFC performance by using multistage operations is discussed in details. Preliminary works consider the systems in which the effect of pressure drop is neglected. Then, more realistic calculations taking into account the effect of pressure are carried out. Details of the study are given in the following sections.

5.1 Model validation

The developed model is validated by comparing with results from the previous work (Eduardo *et al.*, 2005) which is the original reference of several concerning expressions of this work. Fig. 5.1 shows the results of *Power density - Current density* and *Voltage – Current density* curves for the system fed by pure hydrogen as the fuel and air as the oxidant. The cell is operated at a fuel utilization of 80%. The continuous lines show the simulation results from this study while symbols show those from the previous work. Based on the same operating condition, the comparison shows good agreement between those data with small deviation within 4.6%, indicating that our model is capable of predicting the performance of the planar SOFC. It should be noted that the discrepancy may be arisen from our assumption which neglects the effect of concentration overpotential due to mass transport effect, unlike the reference work. It was reported that the concentration overpotential becomes an important loss when the system is operated at low concentration of the reactant gases and high values of current density (Chan *et al.*, 2001). Therefore, to ensure the reliability of our model, the main results in this study are simulated within the range of moderate current density (less than 8000 A/m^2).

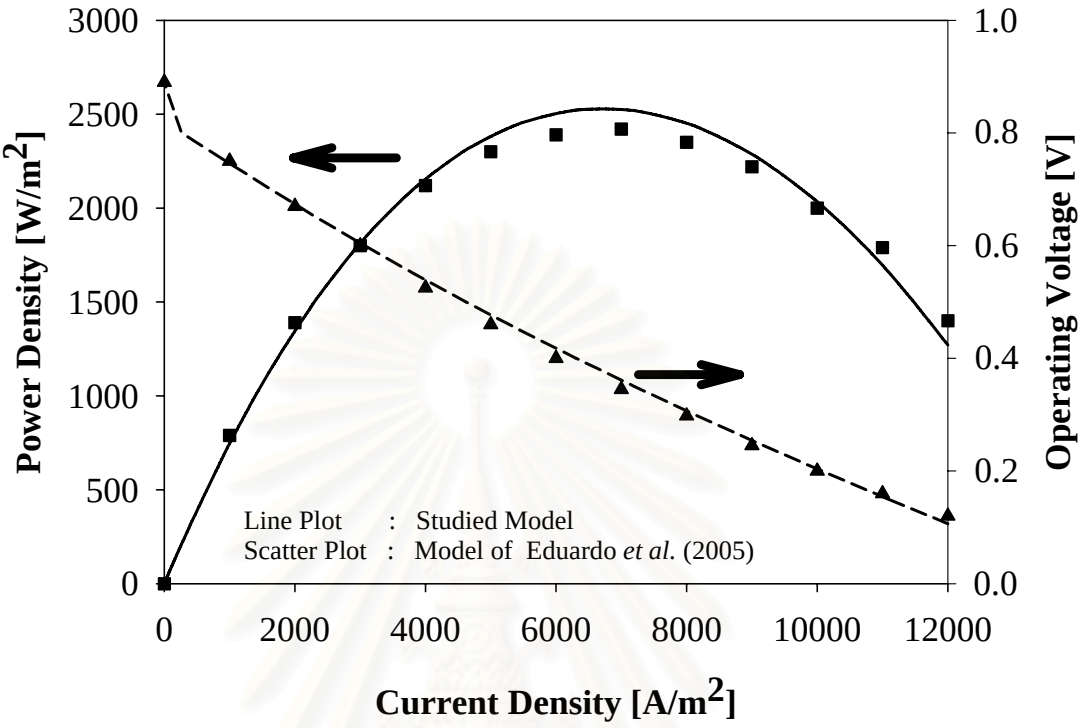

Fig. 5.1 Characteristic curves of SOFC (pure hydrogen as fuel and air as oxidant at fuel utilization = 80% and temperature = 1173 K).

5.2 Performance of single-stack SOFC and multiple stack SOFCs: Neglecting effect of pressure drop

In this section, the ideal models, assuming that the effect of pressure drop is negligible are considered. The study starts with the single-stack SOFC in order to understand effects of important operating parameters (methane feed rate and operating voltage) on SOFC performance (electrical power and efficiency) in a single reference stack. After that, from available optimal operating condition, comparison between conventional SOFC configurations in which multiple stacks are typically arranged in parallel and the alternative ones in which stacks are networked in series is investigated. The operating temperature was kept constant at 1173 K for all simulations.

5.2.1 Performance of the single stack SOFC

It is customary that operating voltage significantly determines the performance of SOFC as shown in Fig. 5.1. In order to show the effect of operating voltage on the generated power of a single SOFC stack, the calculations were based on the same cell area of 1.2 m^2 for one stack. As shown in Fig. 5.2, when the operating voltage increases, the generated power tends to raise at a rate being more or less depending on operating methane feed rate. Until the operating voltage reaches a peak value, the generated power begins to reduce, like the overturned bell curve. For example, at 0.01 mol/s methane feed rate, the maximum power is equal to 3.2 kW when operating voltage is set to 0.46 V. Fig. 5.3 shows on the effect of operating voltage on electrical efficiency in single SOFC stack which corresponds obviously with results of generated power presented above on the basis of the same cell area and methane feed rate. Therefore, it is appropriate to operate in voltage close to this maximum value in order to acquire the optimal power and electrical efficiency.

However, some effect of operating voltage on fuel utilization is also essential to be considered in order to come to a decision on the possibility of operating at any voltage because fuel utilization is generally about 0.8 – 0.95 for s typical SOFC operation (Riensche *et. al.*, 1998). From obtained results, Fig. 5.4 indicates that, at low range of operating voltage, fuel utilization is equal to 1. After that, it begins to have a tendency to decrease. This phenomena takes place because at the beginning of operating voltage before approaching to a changing value, the required cell area, which will raise following the increase of operating voltage, is less than the given cell area. It means that the fuel is consumed completely as a result of excess cell area. While, with operating voltage after that value, the given cell area is not sufficient for the increase of required cell area. Thus, it is not possible to keep its fuel utilization constant. By this reasons, aside from getting the optimal power and electrical efficiency, the operating voltage should be selected carefully as to maintain fuel utilization in acceptable range as mentioned. Sometimes, it may be necessary to adjust methane feed rate as well.

Considering the influence of methane feed rate, Fig. 5.3 indicates that it is favorable to operate the SOFC at low methane feed rate in order to obtain high electrical efficiency. However, in practical case, it is impossible to operate at this condition due to achievement of low generated power as shown in Fig. 5.2. Additionally, at low methane feed rate, it also encounters a problem on narrow range of fuel utilization which is difficult to select suitable operating voltage (Fig. 5.4). Therefore, with complicated decision, the methane feed rate should be recommended being the first significant factor which is selected meticulously, that is, if methane feed rate is a appropriate value, the operating voltage will be chosen more easily.

สถาบันวิทยบริการ
จุฬาลงกรณ์มหาวิทยาลัย

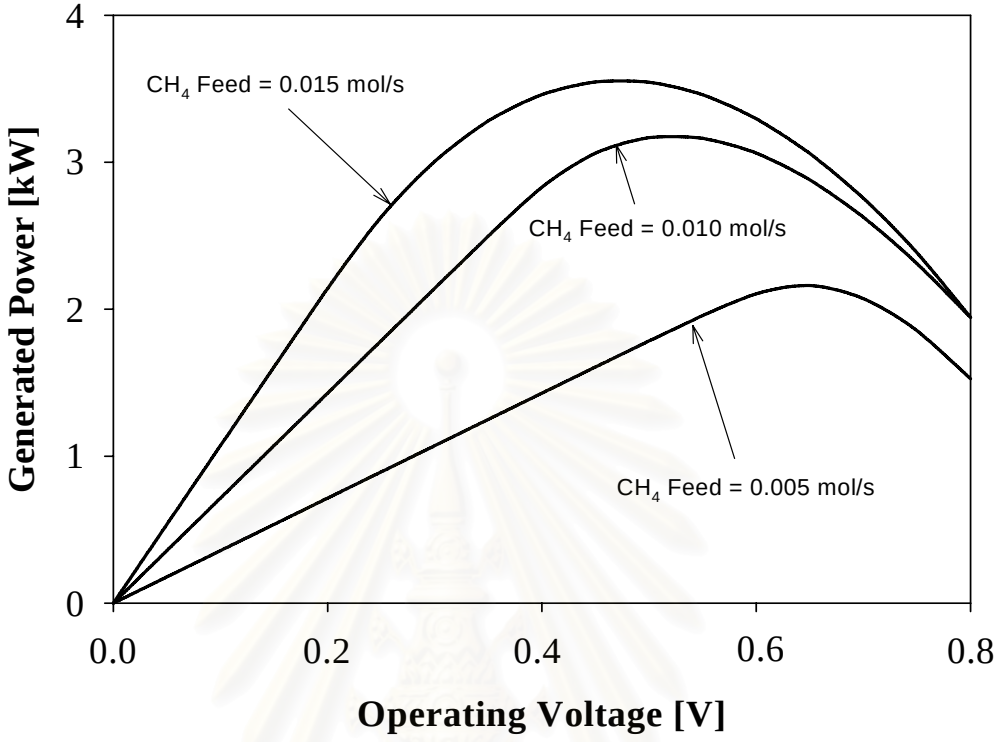

a.)

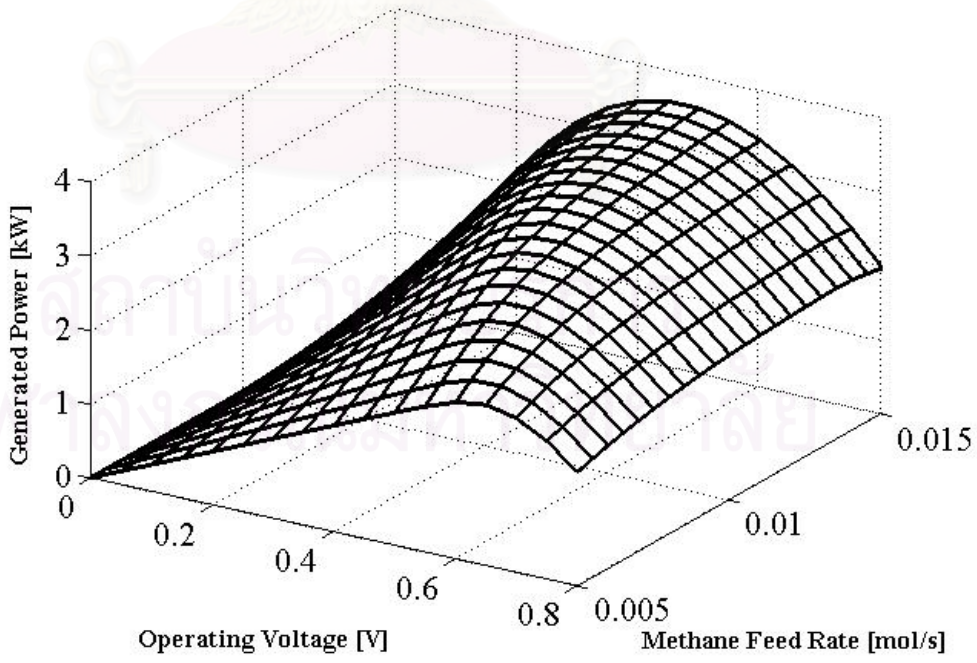

b.)

Fig. 5.2 Effects of methane feed rate and operating voltage on generated power in single SOFC stack (assuming no generated pressure drop).

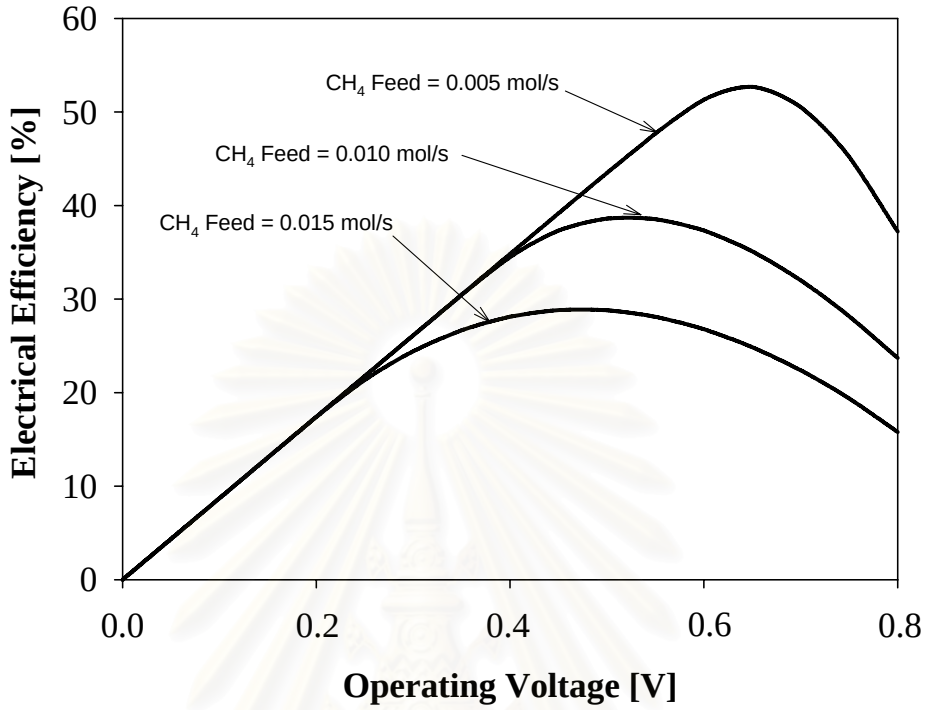

a.)

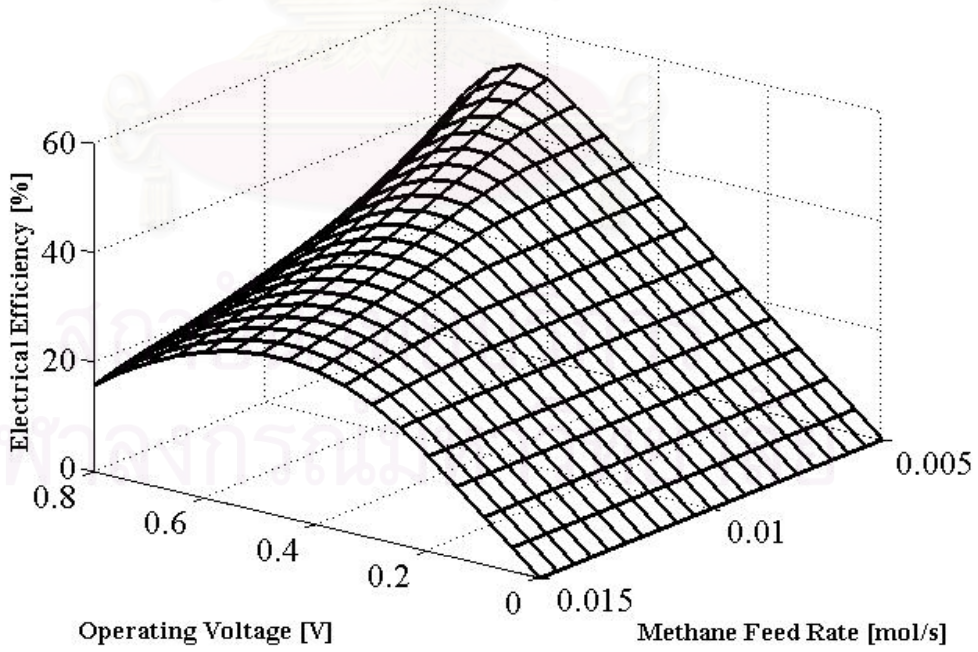

b.)

Fig. 5.3 Effects of methane feed rate and operating voltage on electrical efficiency in single SOFC stack (assuming no generated pressure drop).

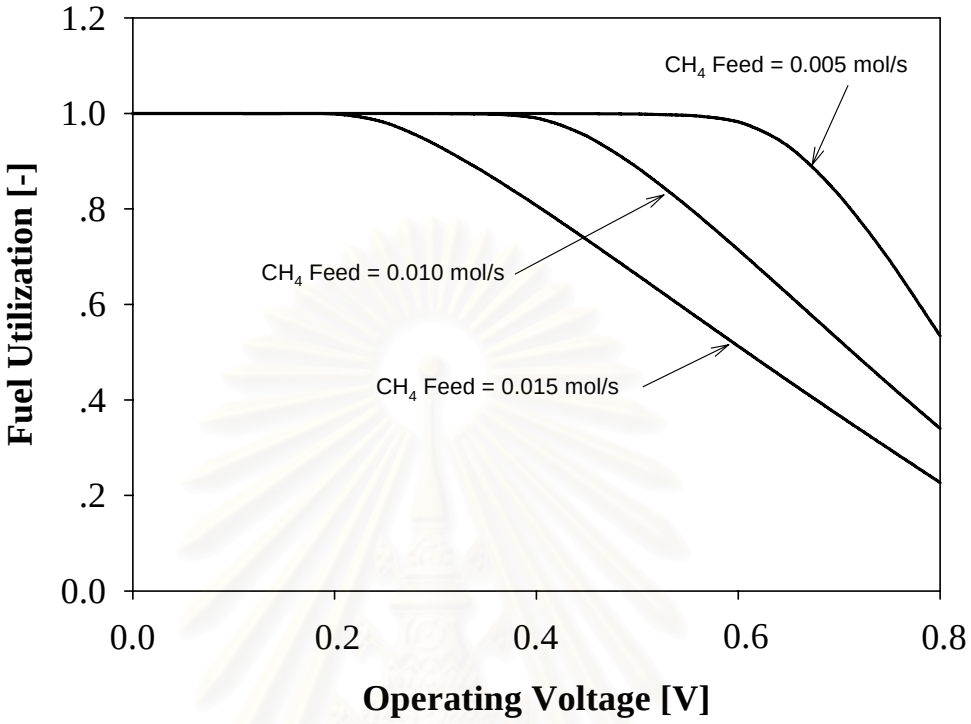

a.)

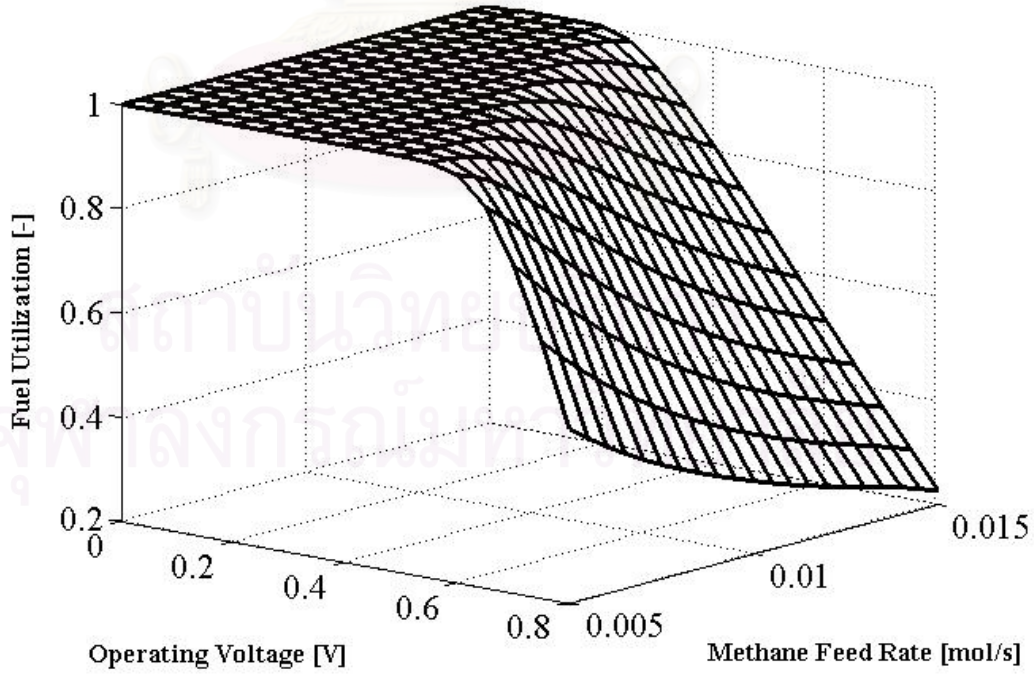

b.)

Fig. 5.4 Effects of methane feed rate and operating voltage on fuel utilization in single SOFC stack (assuming no generated pressure drop.

5.2.2 Performance of multiple stack SOFCs with different arrangement

By suggestion presented above, it indicates the importance of suitable selection of operating condition including operating voltage and methane feed flow in order to confirm the practical feasibility of SOFC. Moreover, the effect of methane feed rate should be taken into the first consideration. Here, it is necessary to select the appropriate methane feed rate following these criterions, accompanied by maximum obtained electrical efficiency and maximum generated power more than 40% and 3 kW, respectively, and widely available operating voltage for the required fuel utilization (0.8 – 0.95) as to be the basic of study in this section. In this work, 0.007 mol/s methane feed rate is selected as basis for any single reference stack.

And then, two or more single stacks at available condition are connected in either parallel or series. The same amount of methane feed rate is fed into external reformer in both arrangements. It will be equal to the methane feed flow rate in single stack multiplied by the number of connected stacks as to keep up the obtained electrical power and efficiency from multiple stack operation not less than the single stack one. In this part, firstly, we compare the results of obtained electrical power and efficiency for two stacks between conventional SOFC arrangement in which multiple stacks are typically arranged in parallel and the alternative one in which stacks are networked in series. After that, the effect of the increase of number of stacks for both conventional and alternative arrangement is investigated in the next section.

สถาบันวิทยบริการ
จุฬาลงกรณ์มหาวิทยาลัย

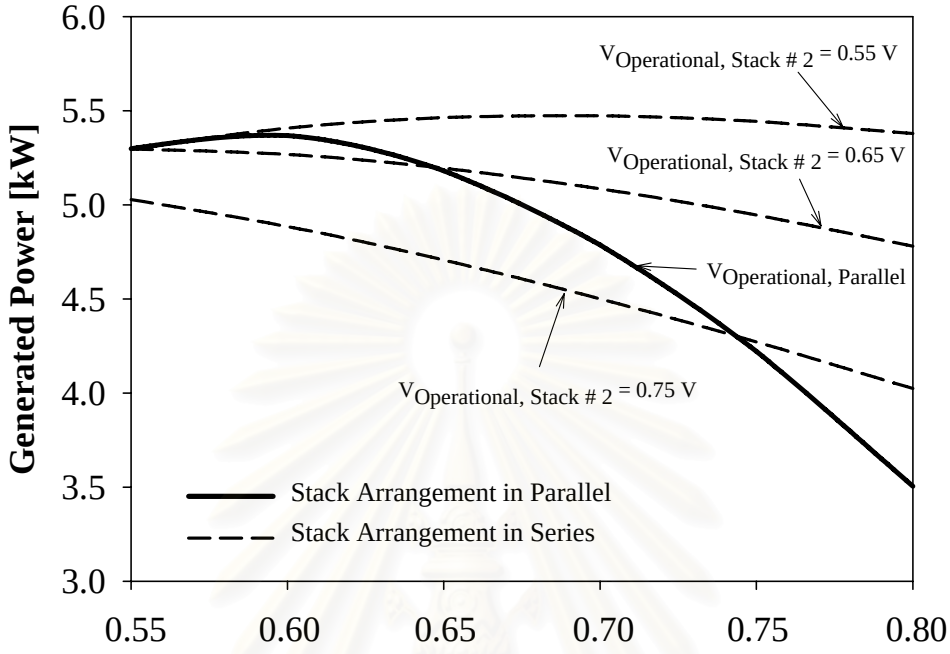

a.)

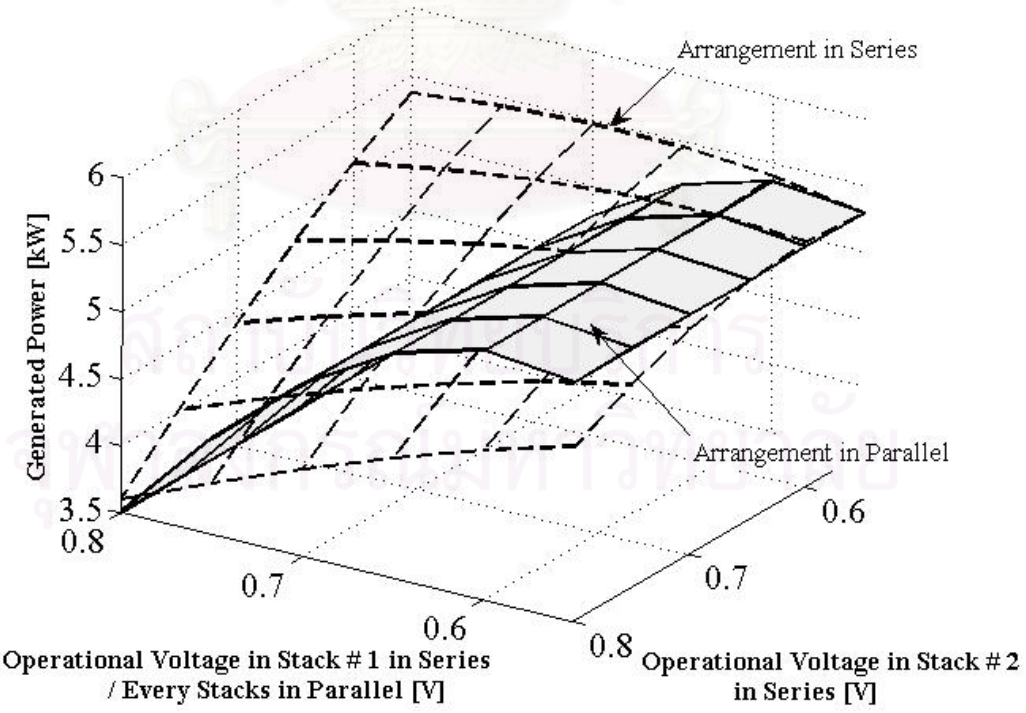

b.)

Fig. 5.5 Relationship of operating voltage in each stack on generated power for arrangement in series and parallel of 2 stacks

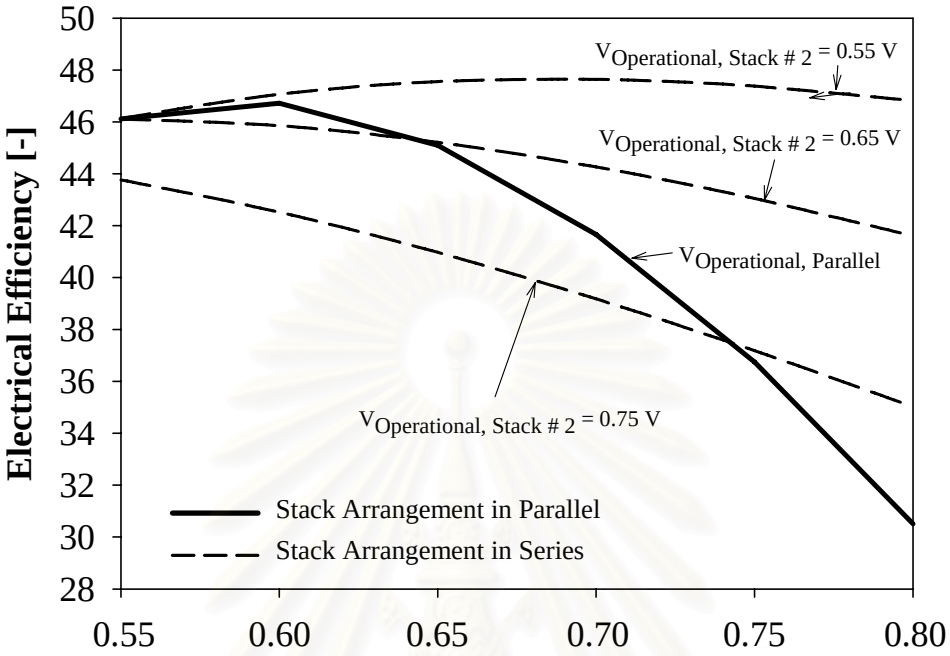

a.)

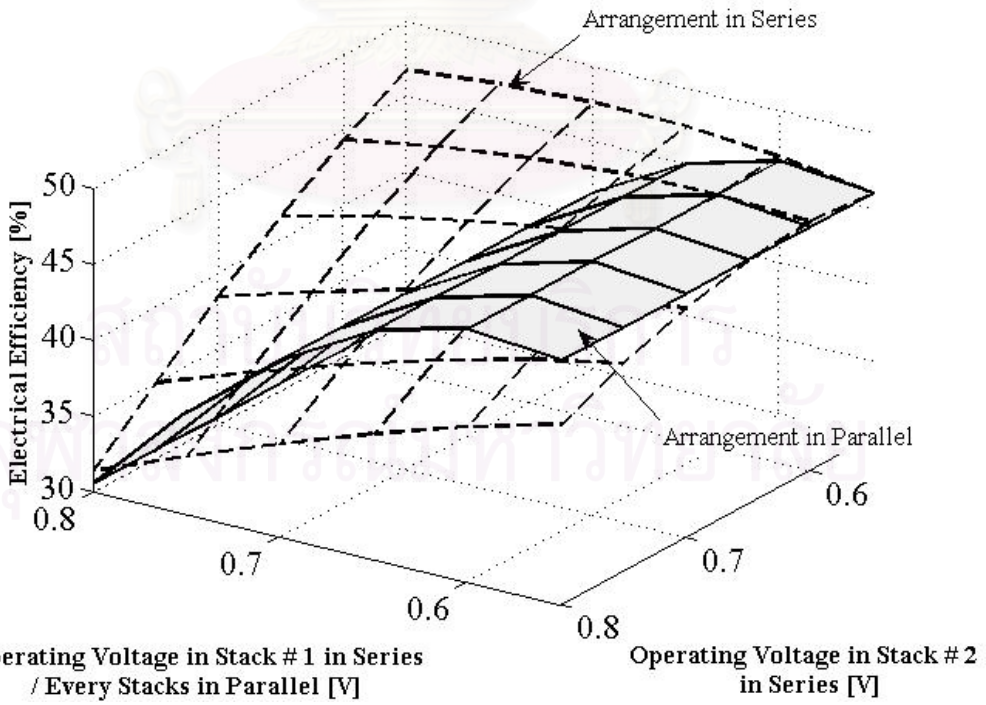

b.)

Fig. 5.6 Relationship of operating voltage in each stack on electrical efficiency for arrangement in series and parallel of 2 stacks

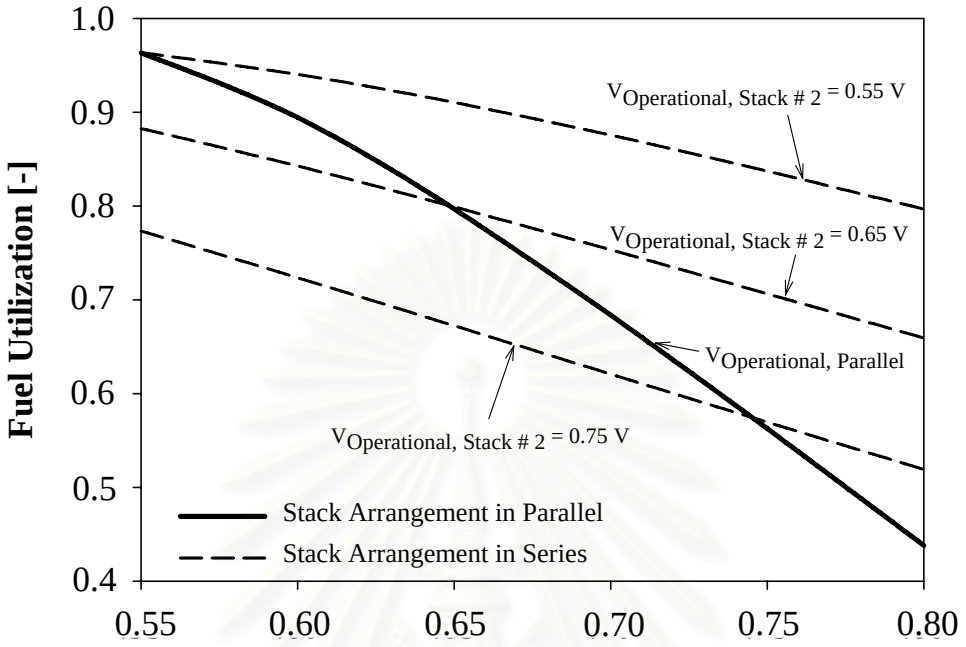

a.)

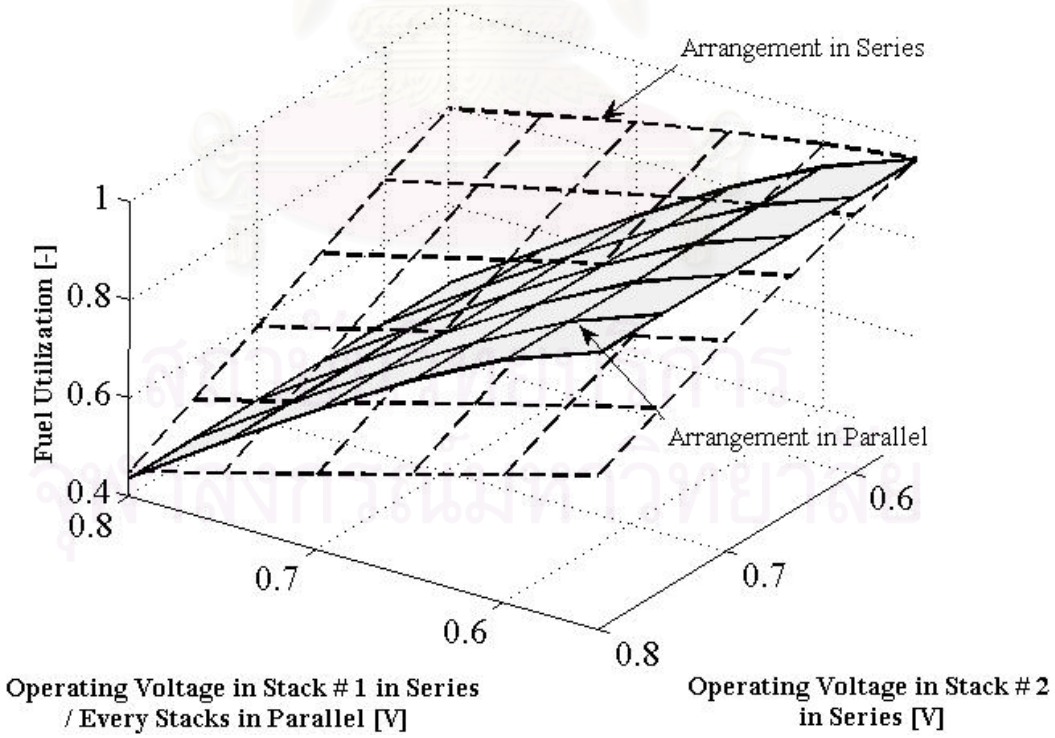

b.)

Fig. 5.7 Relationship of operating voltage in each stack on fuel utilization for arrangement in series and parallel of 2 stacks

Fig. 5.5 compares the generated power between two types of stack arrangements; i.e, parallel, in which operating voltage is equal in every stack, and series arrangement, in which the operating voltage is allowed to vary stack by stack. The thick solid line indicates the results of the arrangement in parallel. It can be observed that there are some ranges of operating voltage in which arrangement in series offers higher generated power than arrangement in parallel (area above of the thick solid line). The same as Fig. 5.6, results of electrical efficiency corresponds obviously with relationship in generated power presented above on the basis of the same operating voltage in each stack. In details of both results, they show that generated power and electrical efficiency of arrangement in series are able to be superior when operating at high voltage differences between the first stack and second stack. Besides, in improvement with arrangement in series, the operating voltage of second stack has always to be lower than the first stack. However, it is still difficult to evaluate the percentage of improved performance if the relationship of operation voltage in each stack on fuel utilization for arrangement in series and parallel is not considered. As shown in Fig. 5.7, it is indicated that a cause of high improvement in arrangement in series at high operating voltage differences between the first stack and second stack takes place partially from higher fuel utilization than the case of arrangement in parallel. Thus, to investigate the percentage of improved performance accurately, it is necessary to compare at the same fuel utilization as to eliminate some suspicion about how many it is possible to keep fuel utilization higher than ever.

For example, at fuel utilization = 0.8, in Fig. 5.7 indicates that operating voltage of arrangement in parallel is about 0.65 V while, another one of arrangement in series is calculated at 0.8 V and 0.55 V for the first and second stacks, respectively. With these operating voltage, in Fig. 5.5 and Fig. 5.6, arrangement in parallel will offer the power at 5.18 kW and electrical efficiency at 45.1% while the power at 5.38 kW and electrical efficiency at 46.8% is obtained in arrangement in series. It is found that the power and electrical efficiency improvement can be achieved as high as 3.8 %.

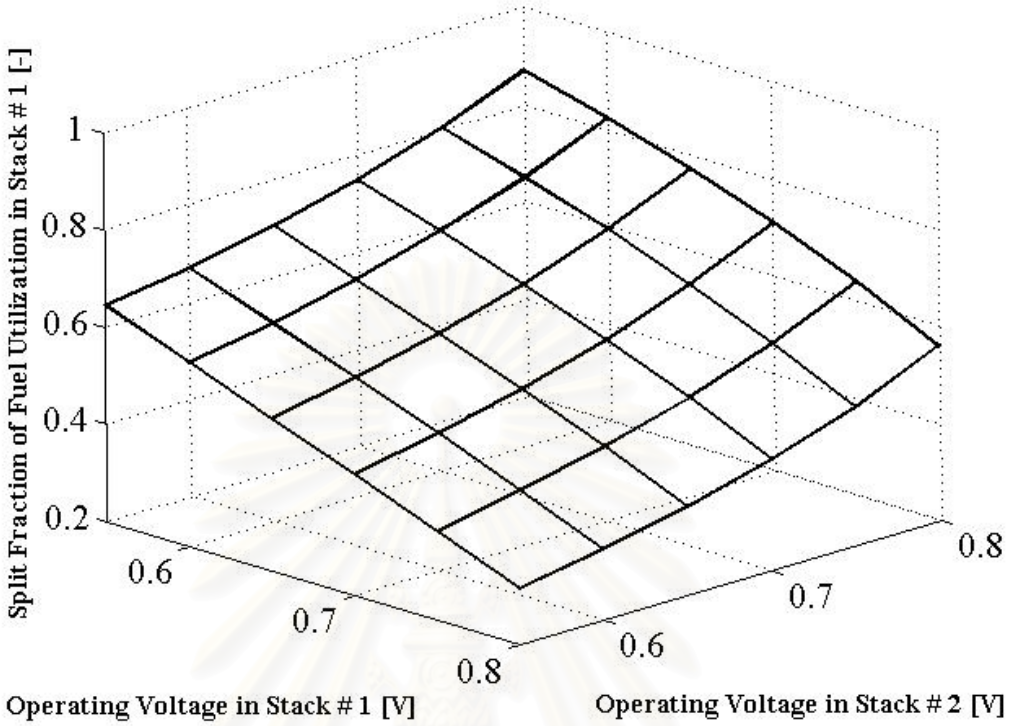

Fig. 5.8 Relationship of operating voltage in each stack of arrangement in series on split fraction of fuel utilization

Fig. 5.8 shows split fraction of fuel utilization, defined as fuel utilization in the first stack divided by final fuel utilization, at different operating voltage in each stack for arrangement in series. It is indicated that in ranges of operating voltage in which arrangement in series offers higher generated power than arrangement in parallel or in ranges of the operating voltage of the second stack higher than the first stack, fuel utilization in the first stack will always be lower than that in the second stack. This means that, in the arrangement in series, performance improvement can be achievable if the second stack is utilized sufficiently.

5.2.3 Influence of number of connected stacks on power improvement by the arrangement in series

From the previous study earlier, the consideration was based on 2 stacks in both arrangements in parallel and series. It is necessary to study further on how the number of increased stacks in arrangement in series affects the percentage of improved power by compared to the case with the arrangement in parallel whose performance is independent of the number of stages. As results of Fig. 5.9, It is observed obviously that the obtained maximum power for arrangement in series tends to increase with the increasing the number of stacks. However, the improvement of arrangement in series will be less significant after the number of stacks more than 2. There are some literatures to report the same observation, that is, these workers suggest and indicate to operate with more than 2 stacks connected in series less attractive (Selimovic and Palsson, 2002, Vivanpatarakij *et. al.*, 2007). Therefore, in the next section of study considering the presence of generated pressure drop, it will consider for 2 stacks SOFC according to the results mentioned above.

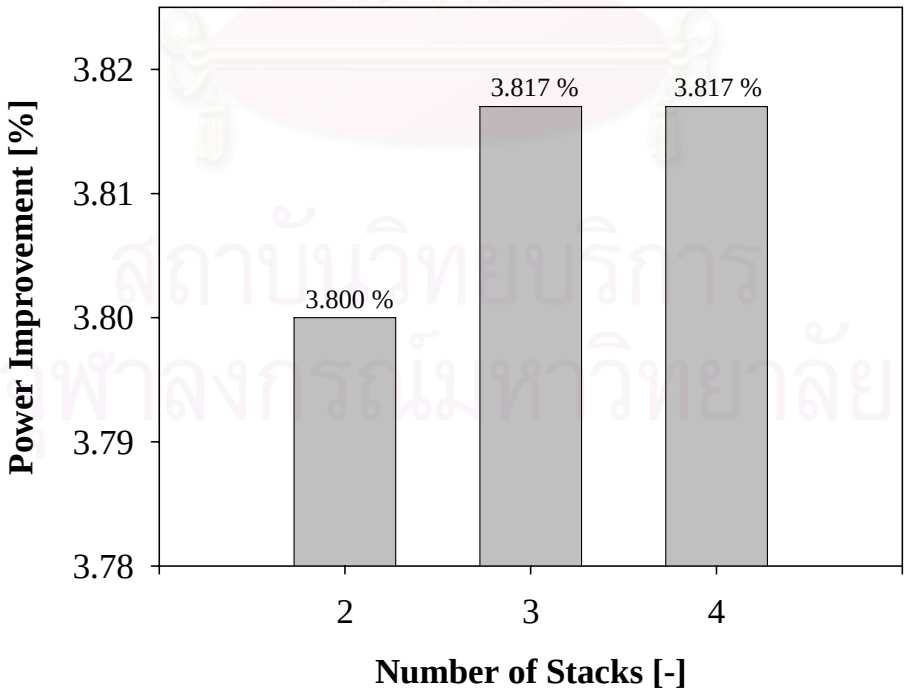

Fig. 5.9 Effect of the number of stacks on the power improvement.

5.3 Performance of SOFCs : taking into account the presence of pressure drop

In this section, the influence of the generated in-stack pressure drop for both conventional and alternative configurations is considered. The pressure drops are calculated in both anodic and cathodic channels based on outlet pressure at atmosphere for which the required inlet pressure of each stack is dependent on operating voltage and stack configuration significantly. Thus, it is necessary to compress both fuel and air to these required inlet pressures by using some compressors. This auxiliary installation specifies that a part of obtained electrical power from SOFC has to be consumed to operate these compressors.

5.3.1 Effect of generated pressure drop on the single stack SOFC performance

From Fig. 5.10, it shows that the anodic gas pressure drop is significantly lower than the cathodic gas pressure drop about a half. This result can be assured with numerical simulation of Joon *et al.* (2002) who calculated the generated pressure drop in both anodic and cathodic channels by varying the channel depth. It is indicated that anodic gas pressure drop is approximately 45-60% of the cathodic gas pressure drop. In this work, it is found that the maximum calculated pressure drops in the anodic and cathodic channels are not higher than 4% and 6% of inlet pressure, respectively. Moreover, it is definite that when the methane feed rate increase, higher pressure drop is observed. Besides, the increase of pressure drop varies directly with operating voltage due to lower fuel utilization at high operating voltage in which the reactant remains more. The next part will indicates the effect of generated pressure drop when comparing with the obtained power from the SOFC in term of the percentage of reduced power from the additional compressor installation. Furthermore, it is observed that, at high operating voltage, the generated pressure drop in the anodic channel increases in rapid rate but not in the cathodic channel which is related with operating voltage in a more linear relationship.

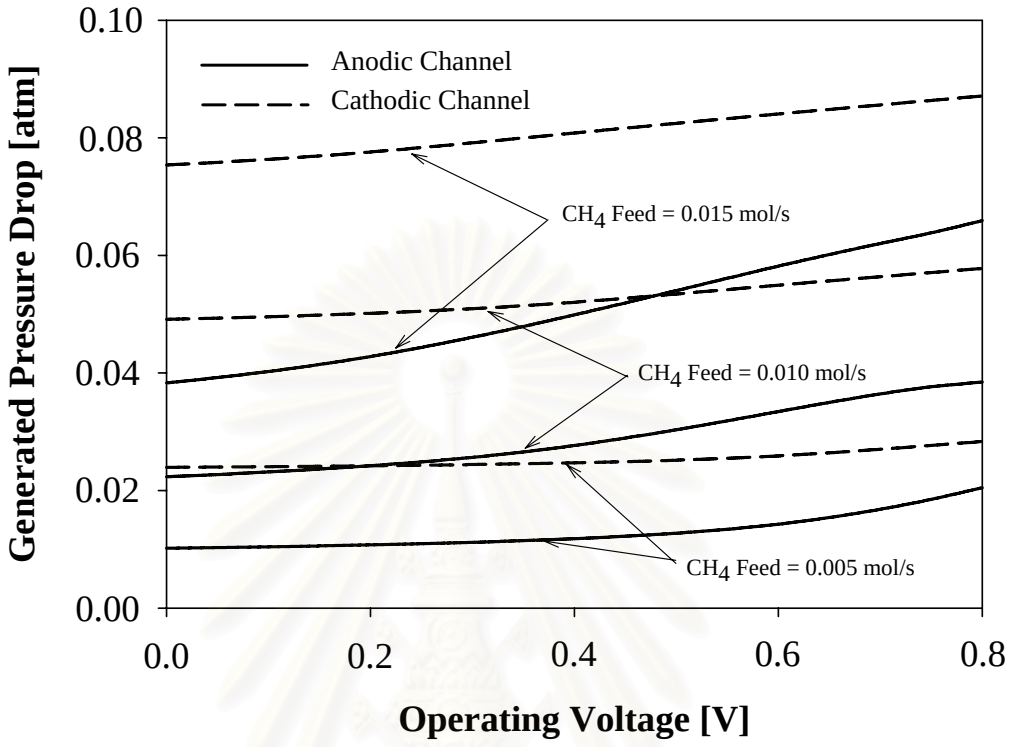

a.)

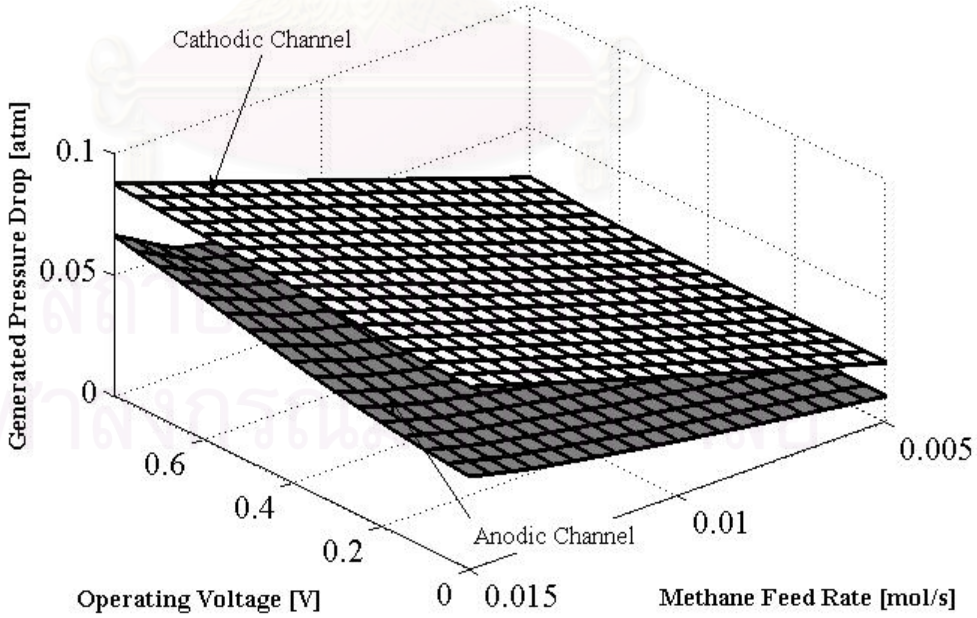

b.)

Fig. 5.10 Effect of operating voltage and methane feed rate on generated pressure drop in the anodic and cathodic channels of the single stack SOFC.

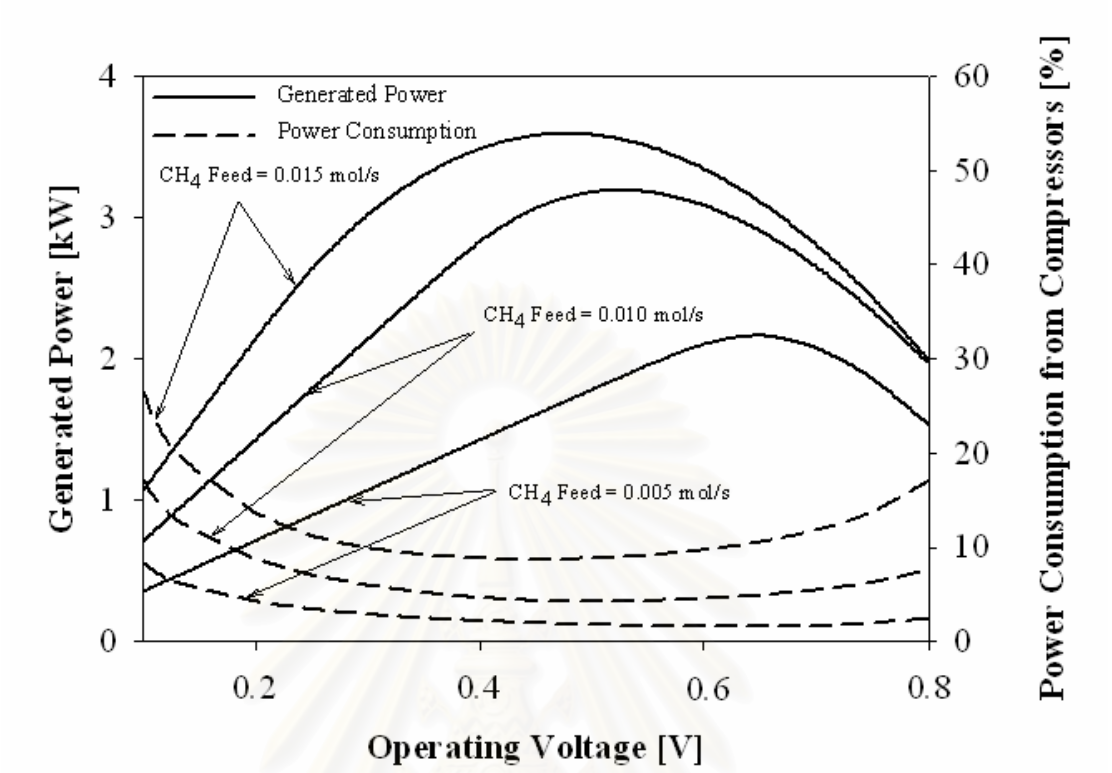

Fig. 5.11 Effect of operating voltage and methane feed rate on generated power from SOFC and power consumption from compressors in single stack

According to the study above, when considering the effect of generated pressure drop, it is essential to compensate this pressure drop to maintain the outlet pressure from cell channels at atmosphere by installation of compressors. Thus, it realizes that a part of obtained power from SOFC has to be consumed by the compressors. Fig. 5.11 shows some effects of operating voltage and methane feed rate on generated power from SOFC and power consumption from compressors in the single stack. Considering the thick solid line, it is found as mentioned that the generated power has a tendency like the overturned bell curve. However, when considering the results of power consumption from the compressor, it is surprising that percentage of power consumption corresponds reversely with the bell curve of the generated power, that is, at the lowest and highest operating voltage, power consumption will increase rapidly. This obviously shows that pressure drop will influence on SOFC more or less, depending on the level of operating voltage and methane feed rate. It is observed that the maximum calculated pressure drops in the

anodic and cathodic channel are quite lower when compared with the inlet pressure. The fraction of energy required on the compressor depends significantly on the operating voltage and methane feed rate. At maximum generated power, the compression power is within the range of 10% of the generated power, indicating that the power consumption from compressor installation is not serious if the obtained power from SOFC is high.

5.3.2 Actual performance of different configurations of integrated stacks and compressors

In this section, it will investigate on three configurations of arrangements of multiple SOFC stacks and compressors by considering the effect of generated pressure drop. SOFC stacks, presented here, will be 2 stacks systems according to the previous calculated results in Section 5.2.3. Performance of each configuration is investigated and compared to propose the best configuration of stack and compressor arrangement that provides optimal electrical power without a reduction of electrical efficiency. Three configurations include:

1.) Configuration A : Multiple stacks are typically arranged in parallel. There is one compressor installed before the conventional SOFC system whose outlet pressure is at atmospheric pressure (Fig. 4.4a).
2.) Configuration B : Multiple stacks are arranged in series. There is only one set of compressor installed at the inlets of the first stack. The outlet pressure is at atmospheric pressure (Fig. 4.4b).
3.) Configuration C : Multiple stacks are arranged in series. There are staged compressors installed at the inlets of each stack. The outlet pressure is at atmospheric pressure (Fig 4.4c).

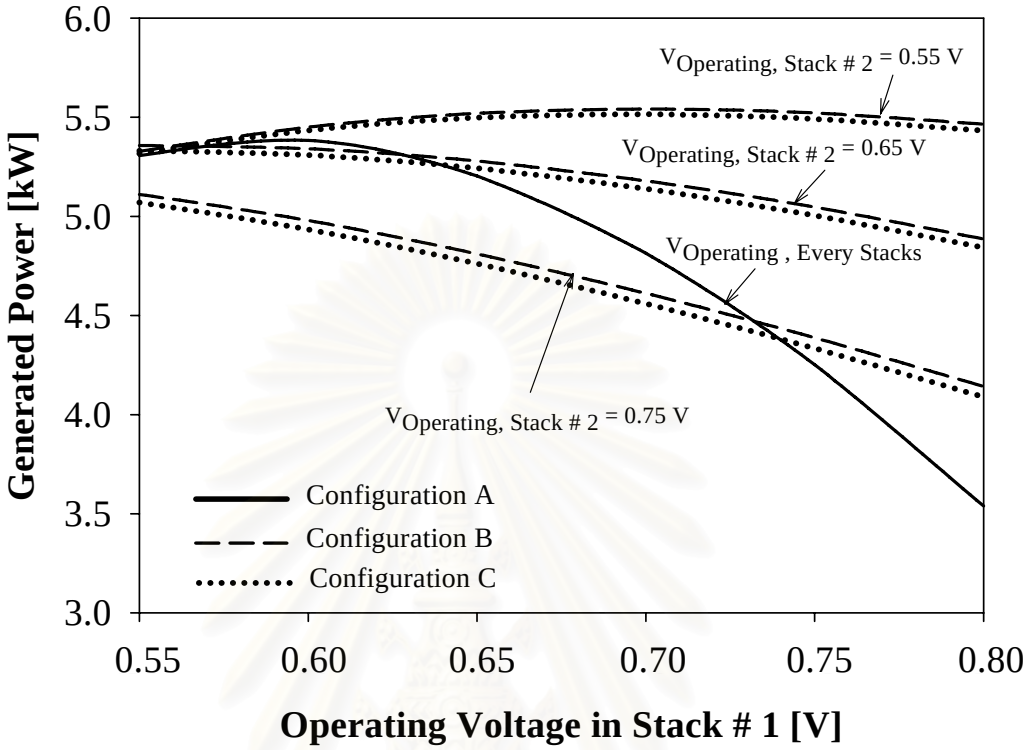

Fig. 5.12 Relationship of operating voltage in each stack on generated power for 2 stacks in different configurations

Fig. 5.12 shows the relationship of operation voltage in each stack on electrical efficiency for the 2 stack SOFC in each configuration. It is assured that there are still some ranges of operating voltage in which the arrangement in series offers higher generated power than the arrangement in parallel. However, for the arrangement in series with two different configurations between stacks and compressors, it indicates that the configuration with one compressor installed at the first inlets of the SOFC system is always able to generate a little more power than another one in which the staged compressors are installed with every SOFC stacks. This result takes place since, in the configuration with one compressor installed only at the inlets of the first stack, it is necessary to compress the fuel and air in higher inlet pressure of the first stack than in the other configuration, in which the fuel and air can be compressed in stack by stack, in order to guarantee the obtained outlet pressure in last stack being at atmospheric pressure. Due to higher pressurized system,

the configuration in series with one set of compressor installed at the inlet of the first stack is preferable to improve its generated power as well as electrical efficiency as shown in Fig. 5.13. However, due to high inlet pressure, it is essential to study some results of power consumption from additional installed compressors when comparing with generated power from SOFC so as to estimate the net power which is an important indicator to investigate the practical feasibility of the use of the best configuration between SOFC stacks arranged in series and compressors. This study in each configuration is presented in the next paragraphs.

.

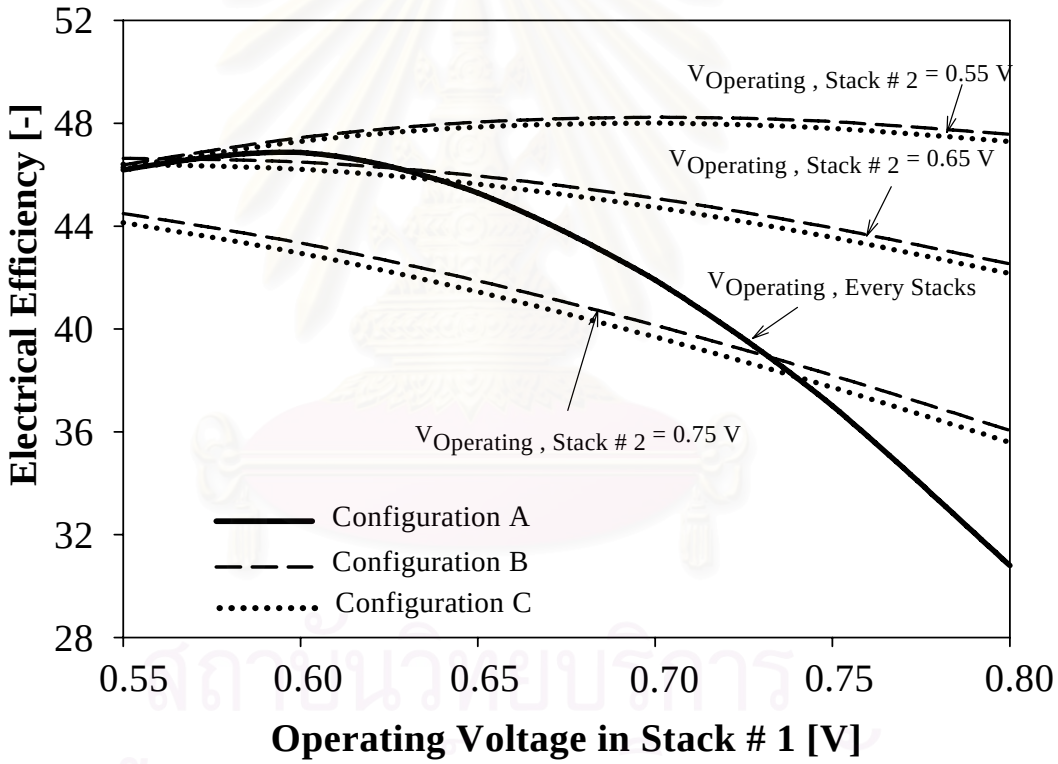

Fig. 5.13 Relationship of operating voltage in each stack on electrical efficiency for 2 stacks in different configurations

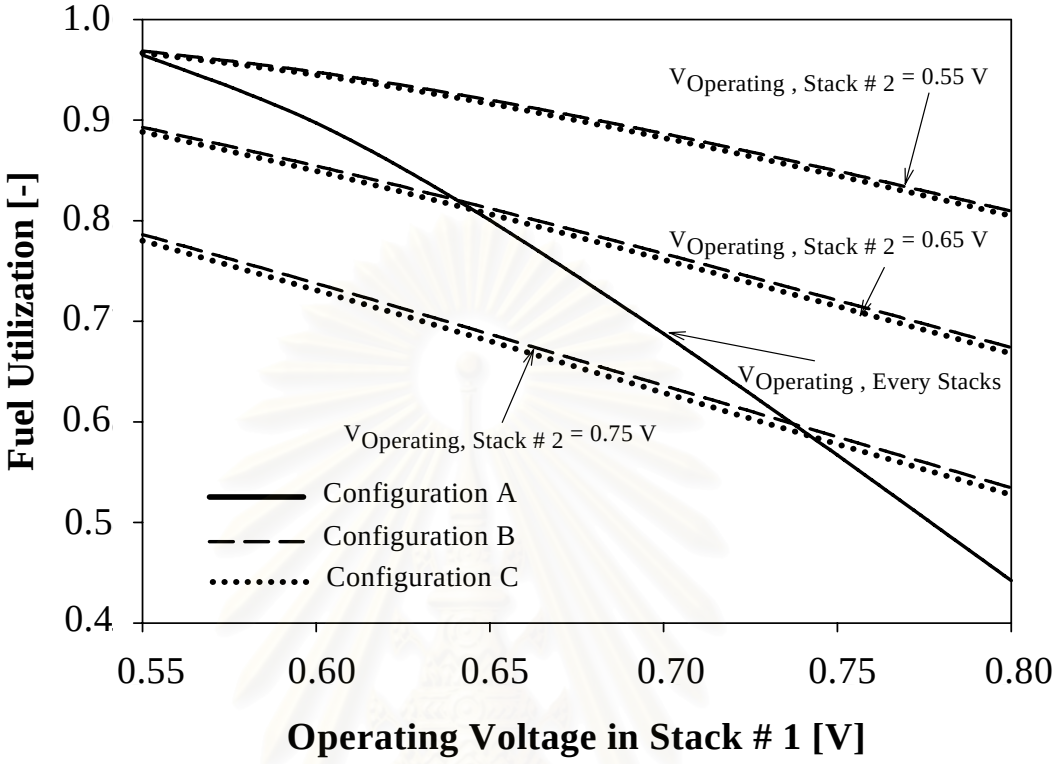

Fig. 5.14 Relationship of operating voltage in each stack on fuel utilization for 2 stacks in different configurations

Refer to Fig. 5.14, this is similar to the previous study in Section 5.2.2. It is still found that the arrangement in series of both configurations can improve fuel utilization well and indifferently. This affects obviously in position direction on several obtained performance. However, to eliminate some suspicion about possibility in the actual operation at high fuel utilization, it is necessary to compare generated power and electrical efficiency in the same fuel utilization in order to show the potential benefit of using the ability of arrangement in series for both configurations on performance improvement of SOFC system accurately. For example, at fuel utilization = 0.8 from Figs. 5.12, 5.13 and 5.14, it is found that the power and electrical efficiency improvement from configuration in series with one compressor installed at the inlet of the first stack can achieve as high as 5.0 %. While the other

one in which the staged compressors are installed with every SOFC stacks can improve only about 4.4%.

Among the three configurations, it is important to understand well that the flow rates of fuel and air streams through stacks networked in series are much larger than those through stacks connected in parallel although the same initial feed streams are used. Since configuration in parallel divide the initial feed streams among many stacks arranged in parallel. While, the initial feed streams in arranging fuel cell stacks in series are not divided, but fed directly into the first of a series of many stacks. From the obtained results in Section 5.3.1, it is indicated that this increased flow rate creates larger pressure drops. Thus, it assures that both configurations in series will encounter on generated pressure drop much more than in parallel as shown in Fig. 5.15. It shows obviously that pressure drop in configurations arranged in series is higher about 4.7 and 3.75 times in the anodic and cathodic channels, respectively, when comparing with the configurations arranged in parallel. However, it still depends on operating voltage in each stack following some causes as mentioned in Section 5.3.1.

Besides, it is found further that the configuration in series with one compressor installed at the inlets of the first stack consumes less power in compressor operation than the other one in which the staged compressors are installed with every SOFC stacks. Due to higher inlet pressure in the first stack of configuration in series with one compressor installed before SOFC system, its fuel utilization in first stack will increase more. This results in the lower generated pressure drop than the other configuration in which the staged compressors are installed with every SOFC stacks. Therefore, it is not surprised that, in the case of stack arrangement in series, configuration in series in which one compressor is installed at the inlets of the first stack is the better option in actual operation because it can obtain the high power with low pressure drop, which will guarantee the power consumption from compressors not to be high.

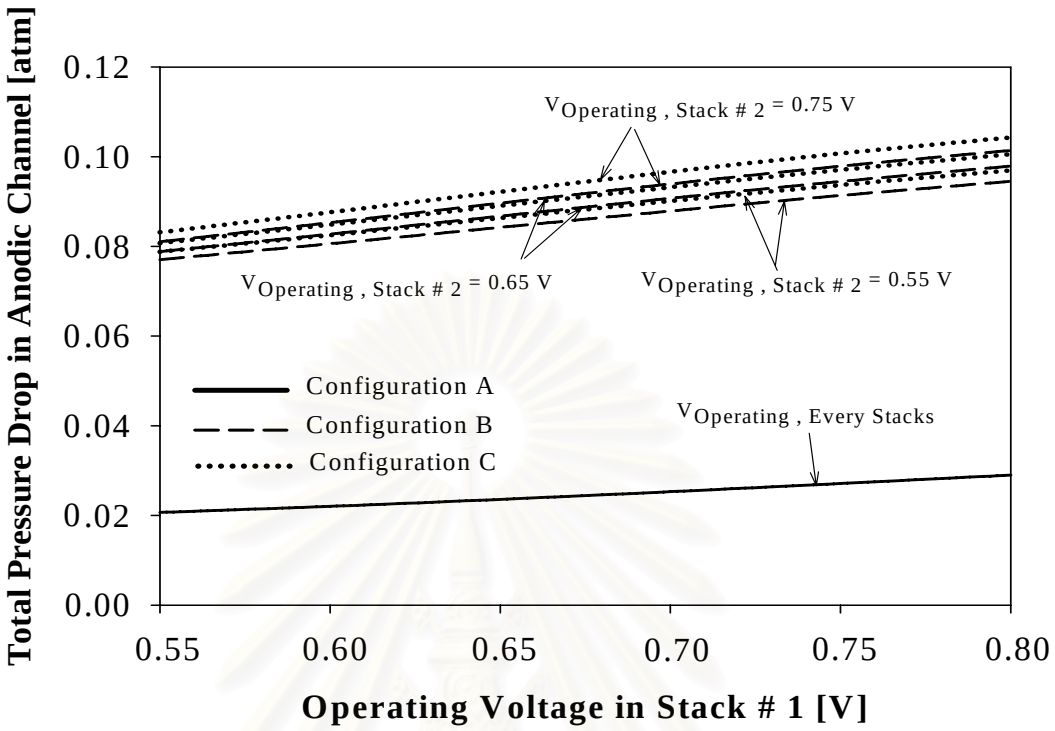

a).

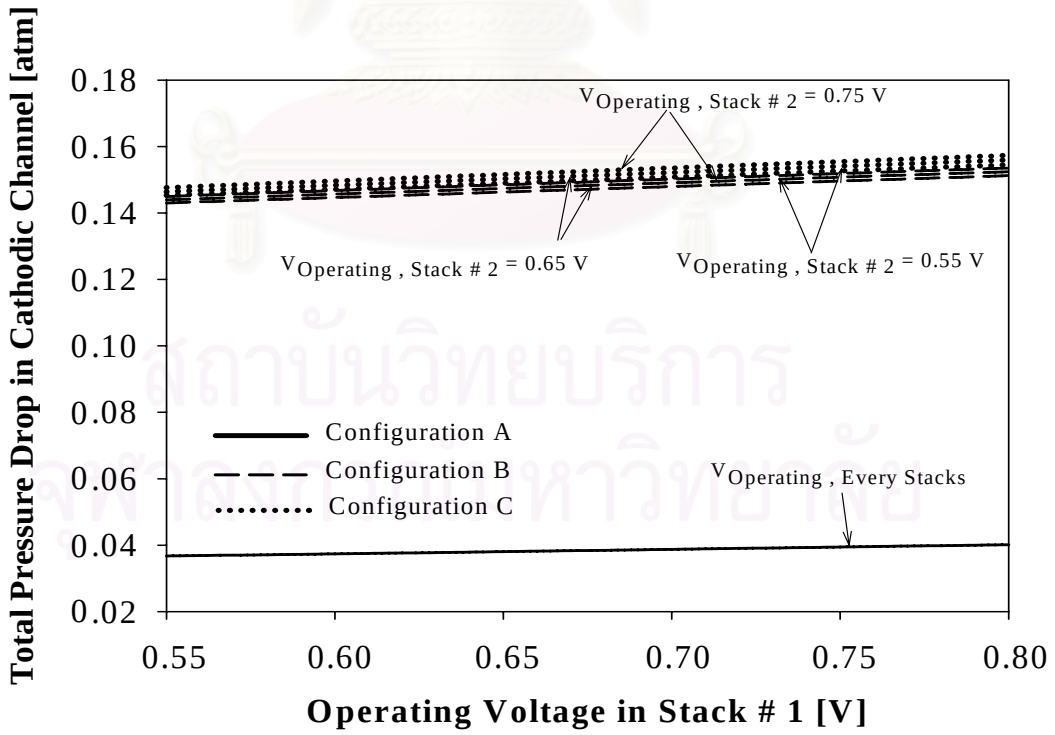

b.)

Fig. 5.15 Effect of operating voltage in each stack on generated pressure drop in anodic and cathodic channel in different configurations

On the other hand, when comparing with case of stack arrangement in parallel in which one compressor is installed at the inlets of the first stack, some power consumption of configuration in series is still much higher. From Fig. 5.16, it is about 5 – 6 times, depending on operating voltage in each stack.

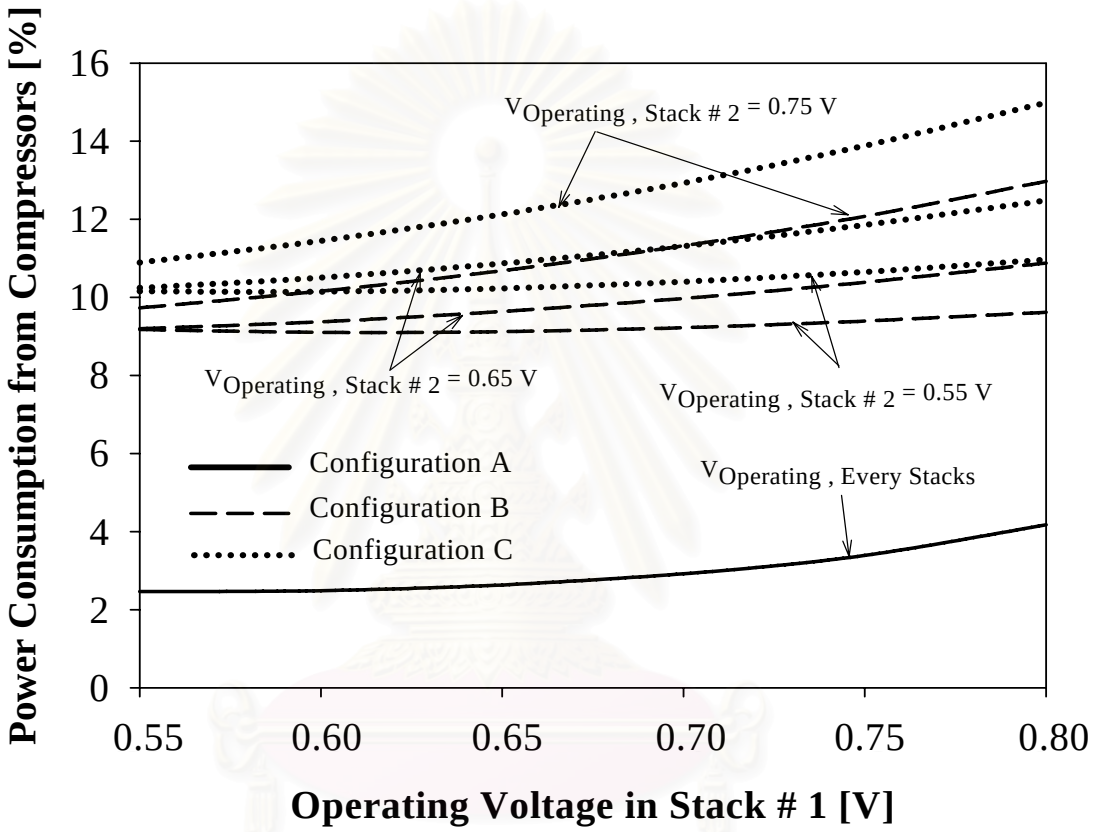

Fig. 5.16 Relationship of operating voltage in each stack on power consumption from compressors for 2 stacks in different configurations

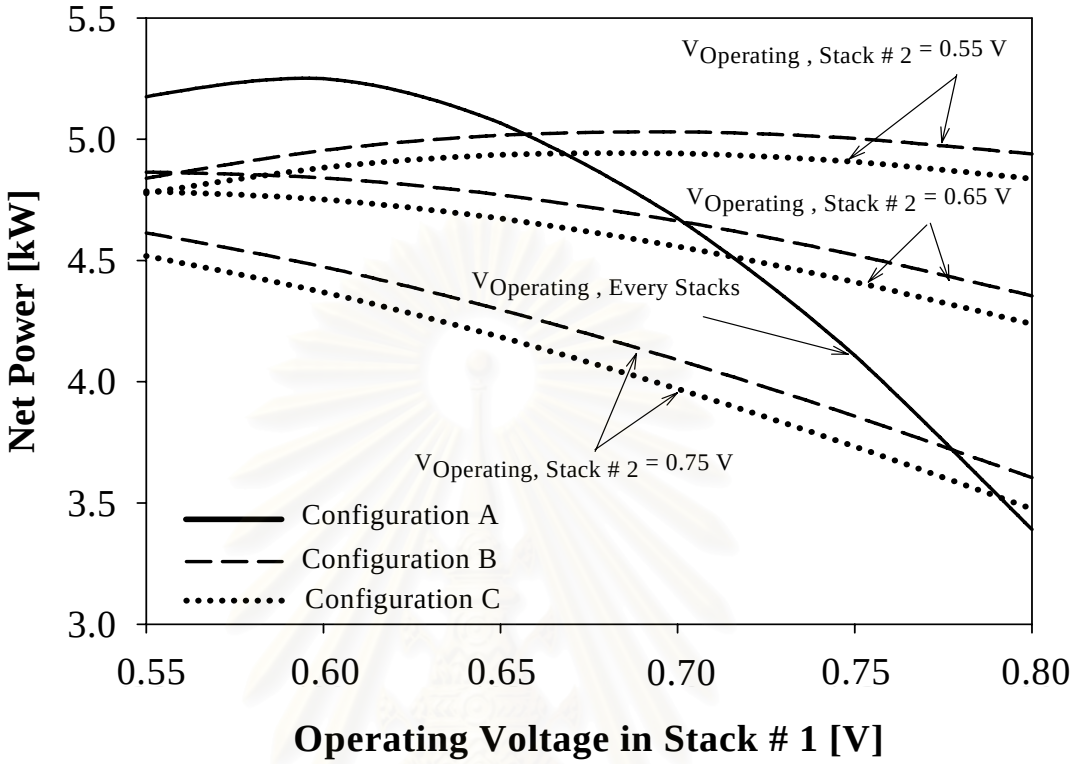

Fig. 5.17 Relationship of operating voltage in each stack on the obtained net power for 2 stacks in different configurations

As there are some contrasts between results of generated power from SOFC and power consumption from compressor in order to propose the best configuration especially in stack arrangement in parallel and series with one compressor installed before the SOFC system, thus, it is necessary to compare and judge by using the total obtained net power. From Fig. 5.17, it is interesting that, when having considered the generated power from SOFC minus power consumption from compressors in each configuration, the obtained net power from the configuration in parallel is the highest in range of operating voltage of configuration in parallel about 0.55 – 0.65 which is corresponding to the range of fuel utilization at 0.8-0.95 as shown in Fig. 5.14. With a higher range of operating voltage in which configuration in series offers higher net power than configuration in parallel, this means understandably that, in these ranges of fuel utilization for which commercial SOFC is maintained, the obtained net power

from configuration in series is not able to improve better than in parallel, although, generated power from SOFC with configuration in series is higher at the same fuel utilization. Since configurations in series encounters some influence of generated pressure drop much more about many times. Power consumption from further installed compressors is so high that configuration in series should not be suggested in actual operation.

By this reason, it is indicated how many it is required to compensate a part of power consumption from installed compressors by using heat recovery system such as gas turbine system as to offer the practical feasibility further in the use of SOFC configuration with stacks arranged in series.

สถาบันวิทยบริการ
จุฬาลงกรณ์มหาวิทยาลัย

CHAPTER VI
CONCLUSIONS AND RECOMMENDATIONS

6.1 Conclusions

This thesis involves several numerical calculations in order to determining potential technical benefit from operating the SOFC with multiple stacks arranged in series over a conventional SOFC operation with stacks arranged in parallel. From the study the following conclusions can be drawn

1. For the simulation results based on the assumption of no pressure drop, it is indicated that, to obtain the optimal performance for a general stack, the methane feed rate and operating voltage should be selected carefully. On this basic, with stack connection in parallel and series at the same number of stacks and fuel utilization, it is found that the power and electrical efficiency improvement by using serially connected stacks can be achieved as high as 3.8 %. However, the improvement of arrangement in series becomes less significant after the number of stacks more than 2.

2. In another study, models take into account the influence of the generated in-stack pressure drop for both conventional and alternative configurations. Based on the outlet pressure at atmospheric pressure, the required inlet pressure of each stack is significantly dependent on operating voltage and stack configuration. From the results of a single stack, it is found that the maximum calculated pressure drops in the anodic and cathodic channels are not higher than 4% and 6% of the inlet pressure, respectively. Thus, when installing some compressors, the problem on the power consumption from compressor installation is not serious if the obtained power from SOFC is high. Moreover, in the case of the increased number of stacks in several configurations, the configuration in series with one compressor installed at the inlets of the first SOFC stack is the best option in the actual operation because it can offer higher power improvement with lower pressure drop than the same configuration in

which the staged compressors are installed before each SOFC stack. The power and electrical efficiency improvement from this configuration can be achieved as high as 5.0%. However the pressure drops still become much more significant as high as 4.7 and 3.75 times in the anodic and cathodic channels, respectively, when compared with the configuration of stacks arranged in parallel. This results in much higher power consumption from the installed compressors of the multiple stack SOFC arranged in series. As a result, the net power from the configuration in series is unable to offer better performance than the one arranged in parallel, although, generated power from the SOFC with the configuration in series is higher at a typical fuel utilization about 0.8-0.95.

6.2 Recommendations

From our previous works, it is recommended to study further on the integration of a heat recovery system such as gas turbine with the multiple stack SOFC arranged in series. This integrated system should offer a good tendency to improve the overall system efficiency. Therefore, more sophisticated models considering energy balance of the SOFC stack and other units should be developed so that the balance of plant of the system could be investigated. A suitable system arrangement and optimum operating condition should be further examined. In addition, economic analysis should also be taken into account in the consideration so that the proposed system could be practical technically and economically.

สถาบันวิทยบริการ
จุฬาลงกรณ์มหาวิทยาลัย

REFERENCES

Aguiar, P., Chadwick, D., Kershenbaum, L. Modelling of an indirect internal reforming solid Oxide fuel cell. *Chemical Engineering Science* **57** (2002): 1665-1677.

Appleby, A.J. and Foulkes, F.R. Fuel Cell Handbook. *Van Nostrand Reinhold.* (1989).

Atkins, P.W. Physical Chemistry, 3rd Edition. *W.H. Freeman and Company*. (1986).

Au, S. F., Woudstra, N., Hemmes, K. Study of multistage oxidation by flowsheet calculations on a combined heat and power molten carbonate fuel cell plant. *Journal of Power Sources* **122** (2003): 28–36.

Badwal, S.P.S and Foger, K. Solid oxide electrolyte fuel cell review. *Ceramics International* **22** (1996): 257-265.

Bessette N.F., Wepfer W.J., Winnick J.A. Mathematical model of a solid oxide fuel cell. Journal of Electrochemical Society **142** (1995):3792–800.

Bradford, M.C.J. and Vannice, M.A**.** CO_2 reforming of CH_4. *Catalysis Reviews - Science and Engineering* **41** (1999): 1-42.

Braun R.J. Optimal Design and Operation of Solid Oxide Fuel Cell Systems for Small-Scale Stationary Applications. Ph.D. Thesis, University of Wisconsin-Madison, Wisconsin. (2002).

Campanari, S. Thermodynamic model and parametric analysis of a tubular SOFC module. *Journal of Power Sources* **92** (2001) 26-34.

Chan. S.H., Khor K.A., Xia Z.T. A complete polarization model of a solid oxide fuel cell and its sensitivity to the change of cell component thickness. *Journal of Power Sources* **93** (2001) 130-140.

Chan, S.H., Low, C.F., Ding, O.L. Simulation of a solid oxide fuel cell power system fed by methane *International Journal of Hydrogen Energy* **30** (2005): 167-179.

Costamagna P, Honegger K. Modeling of solid oxide heat exchanger integrated stacks and simulation at high fuel utilization. Journal of Electrochemical Society **145** (1998): 3995–4007

Conte, M., Iacobazzi, A., Ronchetti, M., Vellone, R. Hydrogen economy for a sustainable development: state-of-the-art and technological perspectives. *Journal of Power Sources.* **100** (2001): 171-187.

Dicks, A.L. Hydrogen generation from natural gas for the fuel cell systems of tomorrow. *Journal of Power Sources.* **61** (2001): 113-124.

Douvartzides, S.L, Coutelieris, F.A., Demin, A.K., Tsiakaras, P.E. Fuel options for solid oxide fuel cell: a Thermodynamic analysis. *AIChE Journal.* **49** (2003): 248-257.

Dunn, S. Hydrogen futures: towards a sustainable energy system. *International Journal of Hydrogen Energy* **27** (2002): 235-264.

Eduardo H.P., Manna M.D., Huttonb P.N., Singha D., Martinb K.E. A cell-level model for a solid oxide fuel cell operated with syngas from a gasification process. *International Journal of Hydrogen Energy* **30** (2005): 1221 – 1233.

Etsell, T.H., Flengas, S.N. Behavior of the liquid silver electrode in a solid- oxide electrolyte concentration cell. *Met Trans* **2** (1971): 2829-2832**.**

George, T. J., and James, R. J. Multi-staged Solid State Fuel Cell Power Plant Concept. *National Energy Technology Laboratory* (1998)

George, T. J., and Smith, W.C. Multi-stage Fuel Cell System Method and Apparatus. *U. S. Patent No. 6,033,794.* (2000)

Heinzel, A, Roes, J., Brandt, H. Increasing the electric efficiency of a fuel cell system by recirculating the anodic offgas. *Journal of Power Sources* **145** (2005): 312–318.

Hirschenhofer, J.H., Stauffer, D.B., Engleman, R.R., Klett, M.G. Fuel Cell Handbook, 5th Edition. *National Energy Technology Laboratory.* (2000).

Ishihara, T., Matsuda, H., Takita, Y. Doped $LaGaO_3$ perovskite type oxide as a new oxide ionic conductor. *Journal of the American Chemical Society* **116** (1994): 3801-3803.

Iwata M., Hikosaka T., Morita M., Iwanari T., Ito K., Onda K.,Esaki Y., Sakaki Y., Nagata S. Performance analysis of planar-type unit SOFC considering current and temperature distributions. Solid State Ionics **132** (2000): 297–308.

Joon H.K., Hai K.S., Young S.Y., Hee C.L. Consideration of numerical simulation parameters and heat transfer models for a molten carbonate fuel cell stack. *Chemical Engineering Journal **87*** (2002): 367–379

Kazim, A. Effect of higher operating pressure on the net change in voltage of a proton exchange membrane fuel cell under various operating conditions. *Journal of Power Sources*. **143** (2005): 9–16.

Khaleel M.A., Lin Z., Singh P., Surdoval W., Collin D. A finite element analysis modeling tool for solid oxide fuel cell development: coupled electrochemistry, thermal and flow analysis in MARC. *Journal of Power Sources*. **130** (2004): 136–148.

Kim, S.D., Hyun, S.H., Moon, J., Kim, J.H., Song, R.H. Fabrication and characterization of anode-supported electrolyte thin films for intermediate temperature solid oxide fuel cells. *Journal of Power Sources.* **139** (2005): 67–72.

Kuchonthara, P., Bhattacharya, S., Tsutsumi, A. Combinations of solid oxide fuel cell and several enhanced gas turbine cycles. *Journal of Power Sources.* **124** (2003): 65–75.

Larminie J, Dicks A. *Fuel cell systems explained.* Wiley (2003).

Li, P.W., Chen, S.P., Chyu, M.K. Novel gas distributors and optimization for high power density in fuel cells. *Journal of Power Sources.* **140** (2005): 311–318.

Liebhafsky, H.A., Cairns, E.J. Fuel Cells and Fuel Batteries. *Wiley*. (1968).

Litzinger, K.P., Veyo, S.E., Shockling, L.A., Lundberg, W.L. Comparative evaluation of SOFC/gas turbine hybrid system options. *ASME Paper GT2005-68909.* (2005).

Massardo, A.F., Lubelli, F. Internal reforming solid oxide fuel cell-gas turbine combined cycles (IRSOFC-GT): Part A- Cell model and cycle thermodynamic analysis. *Journal of Engineering for Gas Turbines and Power.* **122** (2000): 27-35. (2000)

Matsuzaki, Y., Yasuda, I. Electrochemical properties of reduced-temperature SOFCs with mixed ionic-electronic conductors in electrodes and/or interlayers. *Solid State Ion* **152–153** (2002): 463–468.

Mendoza, J.L. Control of emissions of air pollution from non-road diesel engines and fuel. *EPA Public Docket No. A-2001-28* (2002)

Mihn, N.Q. Ceramic Fuel Cells. *Journal of the American Ceramic Society* **76** (1993): 563-588.

Mihn, N.Q. and Takahashi, T. Science and Technology of Ceramic Fuel Cells. *Elsevier*. (1995).

Newman J, Thomas A.K. *Electrochemical systems, Wiley* (2004).

Nielsen, J.R. Catalysis Science and Technology. *Springer-Verlag.* (1983).

Pacheco, E.H., Singh, D., Hutton, P.N., Patel, N., Mann, M.D. A macro-level model for determining the performance characteristics of solid oxide fuel cells. *Journal of Power Sources.* **138** (2004): 174–186.

Palsson, J., Selimovic, A., Sjunnesson, L. Combined solid oxide fuel cell and gas turbine systems for efficient power and heat generation. *Journal of Power Sources*. **86** (2000): 442–448.

Pasaogullari U, Wang C.Y. Computational fluid dynamics modeling of solid oxide fuel cells. *Electrochemical Society Proceeding.* (2003)

Recknagle K.P., Williford R.E., Chick L.A., Rector D.R., Khaleel M.A. Three-dimensional thermo-fluid electrochemical modeling of planar SOFC stacks. *Journal of Power Sources* 113 (2003):109–44.

Riensche, E., Stimming, U., Unverzagt, G. Optimization of a 200 kW SOFC cogeneration power plant: Part I: Variation of process parameters. *Journal of Power Sources* **73** (1998): 251-256.

Sangtongkitcharoen, W., Assabumrungrat, S., Pavarajarn, V., Laosiripojana, N. Praserthdam, P. Comparison of carbon formation boundary in different modes of solid oxide fuel cells fueled by methane. *Journal of Power Sources*. **142** (2005): 75-80.

Selimovic, A., Palsson, J. Networked solid oxide fuel cell stacks combined with a gas turbine cycle. *Journal of Power Sources*. **106** (2002): 76–82.

Senn, S. M., Poulikakos, D. Multistage polymer electrolyte fuel cells based on nonuniform cell potential distribution functions. *Electrochemistry Communications*. **7** (2005): 773–780.

Simner, S.P., Bonnett, J.F., Canfield, N.L., Meinhardt, K.D., Shelton, J.P., Sprenkle, V.L., Stevenson, J.W. Development of lanthanum ferrite SOFC cathodes. *Journal of Power Sources*. **113** (2003): 1–10.

Standaert, F., Hemmes, K., Woudstra, N. Nernst loss and multistage oxidation in fuel cells. *Proceedings of the Fuel Cell Seminar, California.* (1998)

Stoukides, M. Solid-electrolyte membrane reactors: current experience and future outlook. *Catalysis Reviews - Science and Engineering*. **42** (2000): 1-70.

Suwanwarangkul R., Croiset E., Fowler M.W., Douglas P.L., Entchev E., Douglas M.A.. Performance comparison of fick's, dusty-gas and Stefan–Maxwell models to predict the concentration overpotential of a SOFC anode. *Journal of Power Sources*. 122 (2003): 9–18.

Tanaka, K., Wen, C., Yamada, K. Design and evaluation of combined cycle system with solid oxide fuel cell and gas turbine. *Fuel* **79** (2000): 1493–1507.

Tsiakaras, T. and Demin, A., Thermodynamic analysis of solid oxide fuel cell system fueled by ethanol. *Chemical Engineering Science* **102** (2001): 210-217.

Tu, H.Y., Takeda, Y., Imanishi, N., Yamamoto, O. $Ln_{1-x}Sr_xCoO_3$ (L_n = S_m, D_y) for the electrode of solid oxide fuel cells. *Solid State Ion* **117** (1999): 277–281.

Veyo, S.E., Shockling, L.A., Dederer, J.T., Gillett, J.E., Lundberg, W.L. Tubular solid oxide fuel cell/gas turbine hybrid cycle power systems: status. *Trans. ASME Journal of Engineering Gas Turbine Power* **124** (2002): 845–849.

VanderSteen J.D.J., Kenney B., Pharoah J.G., Karan K. Mathematical modeling of the transport phenomena and the chemical/electrochemical reactions in solid oxide fuel cells: a review. *Proceedings of hydrogen and fuel cells 2004*, Toronto. (2004).

Vivanpatarakij S., Assabumrungrat S., Laosiripojana N. Improvement of solid oxide fuel cell performance by using non-uniform potential operation. *Journal of Power Sources* (2007)

Veyo, S.E., Vora, S.D., Litzinger, K.P., Lundberg, W.L. Status of pressurized SOFC/gas turbine power system development at Siemens Westinghouse. *ASME Paper GT2002-30670.* (2002)

Watkiss, P. and Hill, N. The feasibility, costs and markets for hydrogen production *AEA Technology Enviroment.* (2002).

Weber, A., Sauer, B, Muller, A.C., Herbstritt, D., Tiffee, E.I. Oxidation of H_2, CO and methane in SOFC with Ni/YSZ-cermit anodes. *Solid state Ionics* **152** (2002): 543-550.

Wendt H., Kreysa G., *Electrochemical Engineering*, Springer. (1999).

Yakabe H, Ogiwara T, Hishinuma M, Yasuda I. 3-D model calculation for planar SOFC. *Journal of Power Sources*. **102** (2001): 144–54.

Yoon, H.S., Choi, S.W., Lee, D., Kim, B.H. Synthesis and characterization of $Gd_{1-x}Sr_xMnO_3$ cathode for solid oxide fuel cells. *Journal of Power Sources* **93** (2001): 1–7.

Yoon, S.P., Han, J., Nam, S.W., Lim, T.H., Hong, S.A. Improvement of anode performance by surface modification for solid oxide fuel cell running on hydrocarbon fuel. *Journal of Power Sources* **136** (2004): 30–36.

Yoon, S.P., Han J., Nam, S.W., Lim, T.H., Oh, I.H., Hong, S.A., Yoo, Y.S., Lim, H.C. Performance of anode-supported solid oxide fuel cell with $La_{0.85}Sr_{0.15}MnO_3$ cathode modified by sol–gel coating technique *Journal of Power Sources* **106** (2002): 160–166.

Yoon, Y., Kim, M.W., Yoon, Y.S., Kim, S.H. A kinetic study on medium temperature desulfurization using a natural manganese ore. *Chemical Engineering Science* **58** (2003): 2079–2087.

Yoon, Y.G., Lee, W.Y., Park, G.G., Yang, T.H., Kim, C.S. Effects of channel configurations of flow field plates on the performance of a PEMFC. *Electrochimica Acta* **50** (2004): 709–712.

APPENDICES

สถาบันวิทยบริการ
จุฬาลงกรณ์มหาวิทยาลัย

APPENDIX A

SELECTED THERMODYNAMIC AND TRANSPORT PROPERTY DATA

A.1 Thermodynamic properties

Table A.1 Heat capacities of some gases.

Components	$Cp = a + bT + cT^2 + dT^3 + eT^4$ [J/mol]				
	a	b x 10^3	c x 10^5	d x 10^8	e x 10^{13}
Methane	34.942	-39.957	19.184	35.103	393.21
Carbon monoxide	29.556	-6.5807	2.013	-1.2227	22.617
Carbon dioxide	27.437	42.315	-1.9555	0.3997	-2.9872
Water	33.933	-8.4186	2.9906	-1.7825	36.934
Hydrogen	25.399	20.178	-3.8549	3.188	-87.585
Oxygen	29.526	-8.8999	3.8083	-3.2629	88.607
Nitrogen	29.342	-3.5395	1.0076	-0.4312	2.5935

Table A.2 Standard heat of formation ($_{H_f^o}$) and entropy ($_{S_f^o}$) of some gases.

Components	$H^o_f = a + bT + cT^2$ [kJ/mol]			S^o [J/mol.K]
	a	b x 10^3	c x 10^5	
Methane	-63.425	-43.355	1.722	186.27
Carbon monoxide	-112.19	8.1182	-8.0425	197.54
Carbon dioxide	-393.42	0.1591	-0.1395	213.69
Water	-241.8	0	0	188.72
Hydrogen	0	0	0	130.57
Oxygen	0	0	0	205.2

A.2 Transport Properties

Viscosity of pure gases

The viscosity of a pure gas of molecular weight M may be written in terms of the Lennard-Jones parameters as

$$\mu = 2.6693\times10^{-6}\frac{\sqrt{MT}}{\sigma^2\Omega_\mu} \qquad \text{(A.1)}$$

In the form of this equation, if T is (K) and σ is (Å), then μ is unit of kg/m · s. The dimensionless quantity Ω_μ is a slowly varying function of the dimensionless temperature, $\kappa T/\varepsilon$ of the order of magnitude of unity, given in Eq. B-2. It is called the "collision integral for viscosity". The collision integrals have been curve fitted by Neufeld et. al. (1972).

$$\Omega_\mu = \frac{1.16145}{T^{*\,0.14874}} + \frac{0.52487}{\exp\left(0.77320T^*\right)} + \frac{2.16178}{\exp\left(3.89411T^*\right)} \qquad \text{(A.2)}$$

where $T^* = \kappa T/\varepsilon$

Table A.3 Lennard-Jones potential parameters (Hirschfelder *et. al.*, 1964)

Species	σ (Å)	ε/κ (K)
CH_4	3.780	154
O_2	3.433	113
H_2O	3.324	91.56
H_2	2.915	38
CO	3.590	110
CO_2	3.996	190

Viscosity of gas mixture

To calculate the viscosity of a gas mixture, the multicomponent extension of the Chapman-Enskog theory can be used. Alternatively, one can use the following very satisfactory semiempirical formula:

$$\mu_{mix} = \sum_{\alpha=1}^{N} \frac{x_\alpha \mu_\alpha}{\sum_\beta x_\beta \Phi_{\alpha\beta}} \qquad \text{(A.3)}$$

in which the dimensionless quantities $\Phi_{\alpha\beta}$ are:

$$\Phi_{\alpha\beta} = \frac{1}{\sqrt{8}}\left(1+\frac{M_\alpha}{M_\beta}\right)^{-1/2}\left[1+\left(\frac{\mu_\alpha}{\mu_\beta}\right)^{1/2}\left(\frac{M_\beta}{M_\alpha}\right)^{1/4}\right]^2 \qquad \text{(A.4)}$$

Here N is the number of chemical species in the mixture, x_α is the mole fraction of species α, μ_α is the viscosity of pure species at the system temperature and pressure, and M_α is the molecular weight of species α.

สถาบันวิทยบริการ
จุฬาลงกรณ์มหาวิทยาลัย

APPENDIX B

DETERMINING GIBBS ENERGY

B.1 Determination of Gibbs energy (G)

Gibbs energy (G) can be determined at any temperature by equations below:

$$G = H - TS \tag{B.1}$$

$$dG = dH - d(TS) \tag{B.2}$$

Take integration to the above equation:

$$\int dG = \int dH - \int d(TS) \tag{B.3}$$

$$G_T - G_{STD} = \int_{298}^{T} dH - \int_{298}^{T} d(TS) \tag{B.4}$$

where

$$H = H(T) = a + bT + cT^2 \tag{B.5}$$

$$S = S(T) = S^o + \int_{298}^{T} C_p dT \tag{B.6}$$

Where T = temperature within a range of 500 – 1,500 K.

S^o = entropy at standard state (298 K, 1 atm)

สถาบันวิทยบริการ
จุฬาลงกรณ์มหาวิทยาลัย

B.2 Determination of the equilibrium constant (K)

$$G_T = -RT\ln K \quad \text{(B.7)}$$

Rearrange the above equation; $$K = \exp\left(-\frac{G_T}{RT}\right) \quad \text{(B.8)}$$

and from thermodynamic concept $$K = \prod a_i^{v_i} \quad \text{(B.9)}$$

For gas phase system, we can substitute activity with partial pressure term

$$K = \prod\left(\Phi, y_i \frac{P}{P^0}\right)^{v_i} \quad \text{(B.10)}$$

If it is studied at the constant pressure of 1 atm, Equation (B.10) will become the following equation:

$$K = \prod(y_i)^{v_i} \quad \text{(B.11)}$$

From Equation (B.11), the converted moles associated to the reactions involved in the production of hydrogen from steam reforming (x_1, x_2, x_3) can be calculated.

สถาบันวิทยบริการ
จุฬาลงกรณ์มหาวิทยาลัย

APPENDIX C

EXPRESSIONS OF OVERPOTENTIALS

C.1 Activation overpotential

The activation of a chemical reaction involves energy barriers, which must be overcome by the reacting species. These energy barriers are called the activation energy and result in activation or charge transfer polarization. The activation overpotential of an electrochemical reaction is usually expressed by the well-known Butler–Volmer equation:

$$i = i_0\left(\exp\left(\frac{\alpha\eta_{act}\left(n_{BV}F_a\right)}{RT}\right) - \exp\left(\frac{-\left(1-\alpha\right)\eta_{act}\left(n_{BV}F_a\right)}{RT}\right)\right) \qquad \text{(C.1)}$$

Where n_{BV} is the number of electrons transferred in the single elementary rate-limiting step, it is commonly equal to 1 (Chan *et al.*, 2001). The calculation of the activation overvoltage must be performed iteratively since it is not possible to reverse the Butler–Volmer equation. This circumstance is very expensive about the computational point of view but allows avoiding the typical errors yielded by the Tafel equation (Larminie and Dicks, 2002) at current densities, i, lower than the exchange ones. The exchange current densities, i_0 , are the cathodic and anodic electrode reaction rate at the equilibrium potential. A high exchange current density means that good fuel cell performance can be expected. Thus, they could not be handled as constant, since they are dramatically dependent on SOFC operating temperature (Costamagna *et al.*, 2001). The charge transfer coefficient, α, is assumed constant at 0.50, is considered to be the fraction of the change in polarization that leads to a change in the reaction rate constant and its value. With α = 0.5, the activation overpotential can be calculated as follows:

$$i = 2i_0 \sinh\left(\frac{\eta_{act}\left(n_{BV}F_a\right)}{RT}\right) \quad \text{(C.2)}$$

This exchange current density is related to the current density exchanged back and forth when equilibrium is reached and is not easy to evaluate either (Wendt and Kreysa, 1999). Despite this, there is agreement that the following reactions are appropriate for anode (Eq. (C.3)) and cathode (Eq. (C.4)):

$$i_{0,Anode} = 5.5\times10^8\left(\frac{p_{H_2}}{p_{\mathrm{Re}\,f}}\right)\left(\frac{p_{H_2O}}{p_{\mathrm{Re}\,f}}\right)\times\exp\left(\frac{-100\times10^3}{RT}\right) \quad \text{(C.3)}$$

$$i_{0,Cathode} = 7.05\times10^8\left(\frac{p_{O_2}}{p_{\mathrm{Re}\,f}}\right)^{0.25}\times\exp\left(\frac{-120\times10^3}{RT}\right) \quad \text{(C.4)}$$

Pre-exponential factors, exponents and activation energies are taken from tests by Costamagna and Honegger (1998). The complexity of evaluating charge transfer coefficients is applicable to the coefficients involved in Eqs. (C.3) and (C.4).

C.2 Ohmic overpotential

The SOFC operating temperature is high in order to reduce its ohmic losses. This overvoltage is due to: (i) the electrons flow through the anode, cathode and interconnections; (ii) the ionic flow through the electrolyte. The SOFC material resistivity is a temperature-dependent function (Larminie and Dicks, 2002). Usually, the SOFC ohmic resistance is due mostly to the interconnections. Presently, like almost all the papers, the ohmic losses are simulated by means of resistivity, obtained by the experimental temperaturedependent correlations (Calise et al., 2004). Such resistances are summated assuming a series electrical scheme. Ohmic losses through the electrolyte can be reduced by decreasing the electrolyte thickness and/or

improving its ionic conductivity. It obeys to Ohm's law and is expressed by the equation

$$\eta_{ohm} = iR \qquad \text{(C.5)}$$

The resistance of material can calculated from respective resistivity, R which is the function of temperature. (Bessette *et. al.*, 1995)

$$R = \frac{\rho\delta}{A} \qquad \text{(C.6)}$$

Where δ is the component thickness and the ionic conductivity of each component, ρ, can usually be expressed as :

$$\rho = a\exp\left(\frac{b}{T}\right) \qquad \text{(C.7)}$$

For the SOFC considered in this study, the coefficients *a* and *b* of resistivity (Eq. (C.7)) is reported in Table C.1.

Table C.1. Material used and resistivity of cell component.

Material Used	Ni-YSZ / YSZ / LSM-YSZ
Anode Ohmic resistance constant	a = 0.0000298, b = -1392
Cathode Ohmic resistancet constant	a = 0.0000811, b = 600
Electrolyst Ohmic resistancet constant	a = 0.0000294, b = 10350
Interconnect Ohmic resistancet constant	a = 0.0001256, b = 4690

APPENDIX D

CALCULATION OF GAS PHASE ISOTHERMAL PRESSURE DROP

Pressure drop is a term used to describe the change in pressure across a system. The expression for calculating pressure drop of fluid flow in gas phase can be derived from mechanical energy balance. It includes several energy terms:

1.) Elevation potential, $\left(\frac{g}{g_c}\right)z$ where $g_c = 1 \quad kg\ m/N\sec^2$.

2.) Kinetic energy, $\left(\frac{u^2}{2g_c}\right)$.

3.) Internal energy, U .

4.) Work done in crossing the boundary, PV

5.) Work transfer across the boundary, W_s

6.) Heat transfer across the boundary, Q

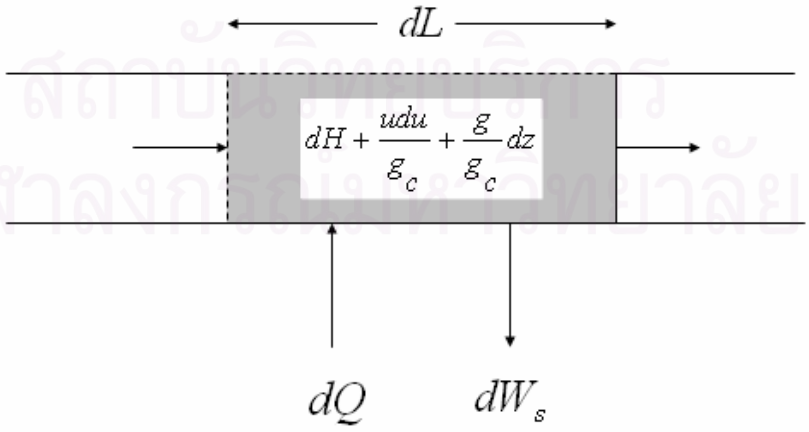

Fig. D.1 The energy balance in any cell channel.

Fig. D.1 shows the energy balance in a small shell from cell channel.

Thus, $$dH + \frac{udu}{g_c} + \frac{g}{g_c}dz = dQ - dW_s \quad \text{(D.1)}$$

Friction is introduced into the energy balance by noting that it is a mechanical process, whose effect is the same as that of an equivalent amount of heat transfer. Moreover, the total effective heat transfer results in a change in entropy of the flowing fluid given by

$$TdS = dQ + dW_f \quad \text{(D.2)}$$

$$dH = VdP + TdS \quad \text{(D.3)}$$

When substitute Eq. (D.3) to Eq. (D.1), the “mechanical energy balance” can be obtained

$$VdP + \frac{udu}{g_c} + \frac{g}{g_c}dz = -\left(dW_s + dW_f\right) \quad \text{(D.4)}$$

For a system of circular cross section, the pressure drop is represented by

$$\Delta P = fp\frac{L}{D}\frac{u^2}{2g_c} \quad \text{(D.5)}$$

Besides, for other shapes and annular spaces, is replaced by the hydraulic diameter

$$D_h = \frac{4(Cross\ Section)}{Wetted\ Perimeter} \quad \text{(D.6)}$$

To determine the friction under laminar regime, the friction is given by the theoretical “Poiseuille” equation

$$f = \frac{64}{\mathrm{Re}} \quad ; \quad \mathrm{Re} < 2100 \quad \text{(D.7)}$$

On the other hand, in turbulent regime, Re > 2100, it is necessary to use data from literature. Olujic (1981). Roorel (1980) proposed a realistic friction expression as follow:

$$f = 1.6364\left[\ln\left(\frac{0.135\varepsilon}{D}+\frac{6.5}{\mathrm{Re}}\right)\right]^{-2} \qquad \text{(D.8)}$$

where, Re is the Reynold number of fluid and ε is roughness.

With the expression from friction, the mechanical energy balance becomes

$$VdP+\frac{udu}{g_c}+\frac{g}{g_c}dz+\frac{fu^2}{2g_cD}dL = -dW_s \qquad \text{(D.9)}$$

In this work, we can apply this expression in form of isothermal flow of uniform ducts by assuming elevation head and work transfer are neglected.

Thus,
$$VdP+\frac{udu}{g_c}+\frac{g}{g_c}dz+\frac{fu^2}{2g_cD}dL = 0 \qquad \text{(D.10)}$$

Make the substitution by

$$u = \frac{G}{\rho} = GV \qquad \text{(D.11)}$$

and the ideal gas relationship

$$V = \frac{P_1V_1}{P} \quad and \quad \frac{dV}{V} = -\frac{dP}{P} \qquad \text{(D.12)}$$

Then, Eq. (D.10) becomes

$$\frac{PdP}{P_1V_1} + \frac{G^2}{g_c}\ln\left(\frac{P_1}{P_2}\right) + \frac{fG^2}{2g_cD}dL = 0 \qquad \text{(D.13)}$$

By integrating each term based on the inlet and outlet conditions, the following expression is obtained.

$$\frac{P_1 - P_2}{2P_1V_1} + \frac{G^2}{g_c}\ln\left(\frac{P_1}{P_2}\right) + \frac{fG^2L}{2g_cD} = 0 \qquad \text{(D.14)}$$

สถาบันวิทยบริการ
จุฬาลงกรณ์มหาวิทยาลัย

APPENDIX E

CALCULATION OF COMPRESSOR POWER CONSUMPTION

Air has to be moved around fuel cell systems for cooling, and to provide oxygen to the cathode. Fuel gas often has to be pumped around the anode side of the fuel cell too. To do this, compressors have to be used. In addition, a part of energy from fuel cell will be consumed in operating compressor. The technology for such equipment is very mature, having already been developed for other applications. The types of compressors used in fuel cell systems are the same as those used in other engines, especially diesel engines. Whatever type of compressor is being used, the symbol used in process flow diagrams is a shown below in Fig. E.1

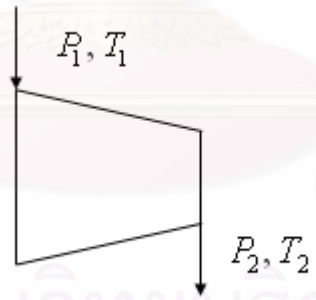

Fig. E.1 Symbol used for compressors.

สถาบันวิทยบริการ
จุฬาลงกรณ์มหาวิทยาลัย

E.1 Compressor Efficiency

Whenever a gas is compresed, work is done on the gas, and so its temperature will rise, unless the compression is done very slowly or there is a lot of cooling. In a reversible process, which is also adiabatic (no heat loss) then it can readily be shown

that if the pressure changes from P_1 to P_2, then the temperature will change from T_1 to $T_2^{'}$, where:

$$\frac{T_2^{'}}{T_1} = \left(\frac{P_2}{P_1}\right)^{\frac{\gamma-1}{\gamma}} \qquad \text{(E.1)}$$

This equation gives the constant entropy, or isentropic temperature change, as is indicated by the $T_2^{'}$. γ is the ratio of the specific heat capacities of the gas, C_p/C_V .

In practice the temperature change will be higher than this. Some of the motion of the moving blades and vanes serves only to raise the temperature of the gas. Also, some of the gas might “churn” around the compressor, doing little but getting hotter. We call the actual new temperature T_2.

To derive the efficiency, we use the ratio between the following two quantities:

- The actual work done to raise the pressure from P_1 to P_2.
- The work that would have been done if the process had been reversible or isentropic – the isentropic work.

To find these two figures we make some assumptions that are generally valid:

- The heat flow from the compressor is negligible.
- The kinetic energy of the gas as it flows into and out of the compressor is negligible, or at least the change is negligible.
- The gas is a “perfect gas”, and so the specific heat at constant pressure, C_p, is constant.

With these assumptions, the work done is simply the change in enthalpy of the gas:

$$W = C_p(T_2 - T_1)m \quad \text{(E.2)}$$

where m is the mass of gas compressed. The isentropic work done is:

$$W' = C_p(T_2' - T_1)m \quad \text{(E.2)}$$

The isentropic efficiency is the ratio of these two quantities. Note that the name “isentropic” does not mean we are saying the process is isentropic, rather we are comparing it with an isentropic process.

$$\eta = \frac{isentropic\ work}{real\ work} = \frac{C_p(T_2' - T_1)m}{C_p(T_2 - T_1)m} \quad \text{(E.3)}$$

and so,

$$\eta_c = \frac{T_2' - T_1}{T_2 - T_1} \quad \text{(E.4)}$$

If we substitute Eq. (E.1) for the isentropic second temperature we get:

$$\eta_c = \frac{T_1}{(T_2 - T_1)}\left(\left(\frac{P_2}{P_1}\right)^{\frac{\gamma-1}{\gamma}} - 1\right) \quad \text{(E.5)}$$

In this derivation we have ignored the difference between the static and the stagnation temperatures. This is important when the gas velocity is high. However, in the fuel cell itself the kinetic energy of the gas is not important. Even in diesel engines, whose flow rates after the compressor are very unsteady, and often rapid, the

equations given here are usually used by presented compressor efficiency in this work at 70 %.

It is useful to rearrange the equation to give the change in temperature:

$$\Delta T = T_2 - T_1 = \frac{T_1}{\eta_c}\left(\left(\frac{P_2}{P_1}\right)^{\frac{\gamma-1}{\gamma}} - 1\right) \quad \text{(E.6)}$$

This definition of efficiency does not consider the work done on the shaft driving the compressor. To bring this in we should also consider the mechanical efficiency η_m, which takes into account the friction in the bearings, or between the rotors and the outer casing if any. In the case of centrifugal and axial compressors this is very high, almost certainly over 98%. We can say then that:

$$\eta_T = \eta_m \cdot \eta_c \quad \text{(E.7)}$$

However, it is the isentropic efficiency η_c that is the most useful, because it tells us how much the temperature rises. For some fuel cell this rise in temperature is useful as it preheats the reactants. On the other hand, for low temperature fuel cells it means the compressed gas needs cooling. Such coolers between a compressor and the user of the gas are called “intercoolers”. We need to know the temperature rise in any case, but Eq. (E.6) also allows us to find the power.

ศูนย์วิทยทรัพยากร
จุฬาลงกรณ์มหาวิทยาลัย

E.2 Compressor Power

The power needed to drive a compressor can be readily found from the change in temperature. If we take unit time, then clearly:

$$Power = \dot{W} = \dot{m} C_p \Delta T \tag{E.8}$$

where $\dot{m}$ is the rate of flow of gas. ΔT is given by Eq. (E.6), and so we have:

$$Power = \dot{m} C_p \frac{T_1}{\eta_c} \left(\left(\frac{P_2}{P_1} \right)^{\frac{\gamma-1}{\gamma}} - 1 \right) \tag{E.9}$$

สถาบันวิทยบริการ
จุฬาลงกรณ์มหาวิทยาลัย

APPENDIX F

SEQUENCE OF THE CALCULATIONS

F.1 Newton's method for solving several unknowns in reformer

In the calculations of reformer model, Newton's method is used to solve several unknowns from equations. This method was applied from Taylor's series expansion to estimate the answers of non-linear equations. The first-order differential equations are considered. Then the equation can be applied as follow:

$$f(x+\Delta x) = f(x)+J(x)\Delta x \tag{F.1}$$

where $J(x)$ is a Jacobian matrix as shown below

$$J(x) = \begin{vmatrix} \frac{\partial f_1(x)}{\partial x_1} & \cdots & \cdots & \frac{\partial f_1(x)}{\partial x_n} \\ \vdots & & & \vdots \\ \vdots & & & \vdots \\ \frac{\partial f_n(x)}{\partial x_1} & \cdots & \cdots & \frac{\partial f_n(x)}{\partial x_n} \end{vmatrix} \tag{F.2}$$

To solve the answers, it is to find Δx which provides:

$$0 = f(x)+J(x)\Delta x \tag{F.3}$$

Δx is calculated by the linear equation below:

$$J(x)\Delta x = -f(x) \tag{F.4}$$

The procedure of the calculation includes:

1. Set the value of $k = 1$
2. If $k \leq N$ (The largest amount of loops in the operation)
   2.1 find $f(x)$ and $J(x)$
   2.2 solve the equation: $J(x)\ \Delta x = - f(x)$ to get Δx
   2.3 set $x = x + \Delta x$
   2.4 $f(\Delta x) <$ *Tolerance of x* or $f(x) <$ *Tolerance of f (x)*, end the calculation
   2.5 set $k = k+1$ and repeat item 2.1
3. If $i > N$, and the answer has not been solved, it would be presumed that the amount of N is too small or the starting value is not appropriate.

F.2 The calculations for SOFC systems

As mentioned in previous chapter, the SOFC system calculations described here were performed using MATLAB software, whereas different SOFC systems are modeled as the single reference stack and arranged reference ones in either parallel or series. This means that the procedure of calculation in each reference stack for both arrangement in parallel and series is not different by simulation code. For basic example of the single stack assuming that the effect of pressure drop is negligible, this procedure of the calculation includes:

1. Set the stack area (*area_set*), operating temperature and operating pressure.
2. Assign the studied value of methane feed rate and operating voltage (*V*).
3. Calculate the inlet fuel flow rate to feed to the SOFC systems from model of reformer using Newton's method and get the excess inlet air flow rate with ratio = 2
4. Set the cumulative current density (*sum_i*) and the cumulative stack area (*sum_area*) = 0.
5. Divide the stack area into 1000 sections (*area_section*)

6. if (*area_set- sum_area*) ≥ tolerance

6.1 Find Electromotive force (E_0) from Nernst equation as follows:

$$E_0 = (RT/(4F))\ln\left(p_{O_2,Cat}/p_{O_2,An}\right) \quad \text{(F.5)}$$

with $$p_{O_2,An} = \left(p_{H_2O,An}/K\,p_{H_2,An}\right)^2 \quad \text{(F.6)}$$

where R is the universal gas constant, T is the absolute temperature, F is the Faraday's constant, p_i is the partial pressure, and K is the equilibrium constant of the hydrogen oxidation reaction.

6.2 When the SOFC is operated at a potential of V, the local current density (i) can be determined according to Eq. (F.7) by iterative method. It should be noted that as the value of E_0 changes along the cell length within the section due to the change in gas compositions, the current density varies within the cell section.

$$\eta_{Ohm}(i) + \eta_{Act,A}(i) + \eta_{Act,C}(i) = E_0 - V \quad \text{(F.7)}$$

where some expressions of overpotentials are shown in Appendix C

6.3 Calculate *sum_area* = *sum_area* + *area_section* and the value of consumed hydrogen in a section from Eq. (4.4).

6.4 Average the obtained current density based on the cumulative stack area.

6.5 Find the additional hydrogen from water gas shift reaction for the next section.

6.6 Calculation the remaining fuel and air flow rate for feeding to the next section and repeat item 6.

7. When calculating completely in all sections, determine the power density and electrical efficiency by Eq. (4.5) and Eq. (4.6).
8. Using the cumulative consumed hydrogen, determine the fuel utilization from Eq. (4.3).

สถาบันวิทยบริการ
จุฬาลงกรณ์มหาวิทยาลัย

VITA

Mr. Nattaphol Ruangrassamee was born on November 17th, 1983 in Bangkok, Thailand. He finished high school from Assumption School Samutprakarn. He received Bachelor's Degree of Engineering in Chemical Engineering from the department of Chemical Engineering, Faculty of Engineering, Chulalongkorn University, Bangkok, Thailand in 2005 and Master's degree of Engineering in Chemical Engineering from the department of Chemical Engineering, Faculty of Engineering, Chulalongkorn University, Bangkok, Thailand in 2007.

สถาบันวิทยบริการ
จุฬาลงกรณ์มหาวิทยาลัย